

## **APPROVAL DOCUMENT**

### **UNIVERSITI MALAYSIA PAHANG FACULTY OF MECHANICAL ENGINEERING**

I hereby declare that the project entitled “*Prototype Development of Normal Asian Human Skull*” is written by *Nurhanis Sofiah bt Abd Ghafar*. I have examined the final copy of this report and in my opinion, it is fully adequate in terms of language standard, and report formatting requirement for the award of the degree of Bachelor of Engineering. We herewith recommend that it be accepted in partial fulfillment of the requirements for the degree of Bachelor of Mechanical Engineering.

(MR. ZULKIFLI BIN AHMAD@MANAP)

Examiner

Signature

PROTOTYPE DEVELOPMENT OF NORMAL  
ASIAN HUMAN SKULL

NURHANIS SOFIAH BT ABD GHAFAR

Report submitted in fulfillment of the requirements  
for the awards of the degree of  
Bachelor of Mechanical Engineering

Faculty of Mechanical Engineering  
UNIVERSITI MALAYSIA PAHANG

JUNE 2013

### **SUPERVISOR'S DECLARATION**

I hereby declare that I have checked this project proposal and in my opinion, this project proposal is adequate in terms of scope and quality of the award of the degree of Bachelor of Mechanical Engineering.

Signature : .....

Name of Supervisor : MR NASRUL HADI BIN JOHARI

Position : LECTURER

Date : 27 JUNE 2013

### STUDENT'S DECLARATION

I hereby declare that the work in this project is my own except for quotations and summaries which have been duly acknowledge. The project has not been accepted for any degree and is not concurrently submitted for award of other degree.

Signature : .....

Name : NURHANIS SOFIAH BT ABD GHAFAR

ID Number : MG09010

Date : 28 JUNE 2013

Dedicated to My Beloved Family

**ABD GHAFAR BIN AWANG**

**ROSIAH BT JUSOH**

**NUR IZZATI BT ABD GHAFAR**

**AHMAD MUBASYIR BIN ABD GHAFAR**

**NUR AKILAH BT ABD GHAFAR**

**NUR AMNI MARDHIAH BT ABD GHAFAR**

## ACKNOWLEDGEMENTS

Assalamualaikum W.B.T and Alhamdulillah for this achievement. I am grateful and would like to express my sincere gratitude to my supervisor, Mr Nasrul Hadi bin Johari for his germinal ideas, invaluable guidance, continuous encouragement and constants support in making this research possible. I appreciate his consistent support and truly grateful for his progressive vision about my training in sciences, his tolerance of my naïve mistakes, and his commitment to my future career. I also would like to express very special thanks to my co-supervisor Mr Hasnun Arif bin Hassan for his suggestions and co-operations throughout the study.

My sincere thanks go to all my lab mates and members of the staff of the Mechanical Engineering Department, UMP, who helped me in many ways and made my stay at UMP pleasant and unforgettable. This gratitude also go to all staffs and lecturer of Centre for Sports Engineering (CenSE) UMP that include Dr Kumaran Kardigama, Prof. Dr. Zahari Taha, Mr. Zulkifli bin Manan, Mr. Azrul Hisham and Dr Zakri bin Ghazali. Last but not least, to my lecturer, Dr Gan Leong Ming who always gives me many ideas regarding fabrication in this project. Many special thanks go to member of CenSE research group for their excellent co-operation, inspirations and supports during this study.

I acknowledge my sincere indebtedness and gratitude to my parents, Abd Ghafar bin Awang and Rosiah bt Jusoh for their love, dream, and sacrifice throughout my life. I cannot find the appropriate words that could properly describe my appreciation for their devotion, support and faith in my ability to attain my goals. Special thanks should be given to my committee members and good friends Siti Nurhidayah bt Daud, Nur Syazwani Mohd Noor, Norasyikin bt Nor Tuah and Muhammad Syarifuddin bin Sulaiman. I would like to acknowledge their comments and suggestions, which was crucial for the successful completion of this study.

## ABSTRACT

Skull which is cover with scalp is skeletal structure of human's head that protect and form a cavity for the brain, where the nervous system is. Nowadays, prototype of human's skull model needed in wide use such as to educate and train physicians, inform patient, support R&D and for surgical planning. The purpose of this study is to build a three dimensional of normal Asian human's skull by using any applicable machine. The process of replicating human's skull start with two dimensional Computed Tomography(CT) data that need to be translate into three dimensional rapid prototyping data by using MIMICS software. The three dimensional(3D) skull model need to be observed and measure as the scope of this project focused to specific normal Asian human. The observation of its morphological features of the skull and linear measurement had found that the 3D skull model belong to normal Asian human. Then, the 3D file images will be exported into related software for fabrication of prototype process. The prototype development had be done by using modeler machine that use subtractive concept. The skull prototype that made up from chemical wood, or its specific name, miraboard 700 undergoes drop ball experiment for capability determination of the skull prototype. For validation, the drop ball test experiment result was compare to result of analytical method. The research comes out with almost the same value percentage different between the experimental and analytical method.

## ABSTRAK

Tengkorak yang diliputi kulit kepala adalah merupakan rangka kepala manusia yang berfungsi untuk melindungi dan menghasilkan kaviti untuk otak dimana terdapatnya sistem saraf. Kini, prototaip tengkorak adalah diperlukan secara meluas bagi tujuan pendidikan, latihan ahli fizik, pemberitahuan kepada pesakit, menyokong kajian dan pembangunan dan rancangan untuk pembedahan. Tujuan kajian ini adalah untuk membina sebuah prototaip tengkorak untuk orang Asia yang normal. Proses membina prototaip ini bermula dengan imej dua dimensi daripada imbasan komputasi tomografi. yang akan ditukar kepada imej tiga dimensi menggunakan program khusus yang dikenali sebagai MIMICS. Imej tengkorak tersebut mesti menjalani proses pemerhatian dan pengukuran bagi memastikan ianya mencapai objektif projek, iaitu menghasilkan tengkorak untuk orang Asia normal. Seterusnya, imej tersebut akan dieksport didalam format STL kepada program yang berkaitan untuk proses pembinaan. Proses pembinaan tengkorak ini telah disiapkan menggunakan mesin modeler, yang menggunakan proses penolakan. Prototaip tengkorak ini yang diperbuat dripada kayu kimia, atau nama spesifiknya adalah miraboard 700 akan menjalani eksperimen impak kepala bagi mengenalpasti kemampuannya berbanding prototaip tengkorak yang lain. Untuk proses pengesahan, keputusan eksperimen telah dibandingkan dengan keputusan yang menggunakan kaedah analisis. Kajian ini telah mendapati peratusan perbezaan yang hampir sama berbanding keputusan eksperimen dan kaedah analisis.



## TABLE OF CONTENT

		<b>Page</b>
<b>EXAMINER APPROVAL DOCUMENT</b>		<b>i</b>
<b>TITLE PAGE</b>		<b>ii</b>
<b>SUPERVISOR'S DECLARATION</b>		<b>iii</b>
<b>STUDENT'S DECLARATION</b>		<b>iv</b>
<b>DEDICATION</b>		<b>v</b>
<b>ACKNOWLEDGEMENTS</b>		<b>vi</b>
<b>ABSTRACT</b>		<b>vii</b>
<b>ABSTRAK</b>		<b>viii</b>
<b>TABLE OF CONTENT</b>		<b>ix</b>
<b>LIST OF TABLES</b>		<b>xiii</b>
<b>LIST OF FIGURES</b>		<b>xiv</b>
<b>LIST OF SYMBOLS</b>		<b>xvii</b>
<b>LIST OF ABBREVIATIONS</b>		<b>xviii</b>
<b>CHAPTER 1            INTRODUCTION</b>		
1.1	Background of The Study	1
1.2	Problem Statement	2
1.3	Objective of Study	3
1.4	Scope of Study	3
1.5	Report Arrangement	4
<b>CHAPTER 2            LITERATURE REVIEW</b>		
2.1	Introduction	5
2.2	Anatomy of Human Head	5
	2.2.1            The Skull	5
	2.2.2            The Brain	7
2.3	Assessment of Race from Skull	8
	2.3.1            Determination of Asian Race Skull	9

2.4	Rapid Prototyping Process	13
2.5	Source of Rapid Prototyping Data for Human Anatomy- CT Scan/MRI	15
2.6	Accuracy of Rapid Prototyping Skull Model	17
2.7	Landmarks of Skull for Linear Measurement Guidelines	20
2.8	Previous Research of Prototype Skull/Head Development	23
	2.8.1 On the use of a patient-specific rapid-prototyped model to simulate the response of the human head to impact and comparison with analytical and finite element models, E.A.C. Johnson and P.G. Young (2005)	23
	2.8.2 Material Modeling and Analysis for the Development of a Realistic Blast Headform, S. G. M. Hossain (2010)	28
2.9	Summary	32

### **CHAPTER 3            METHODOLOGY**

3.1	Introduction	33
3.2	Flow Chart	34
3.3	Design of Project Study	35
3.4	Raw Data from CT scan Images	36
3.5	Extract Region of Interest Process	37
3.6	Fabrication: Prototype Development Process	38
3.7	Experiment: Drop Ball Test	42
	3.7.2            Equipment used for experiment	42
3.8	Conclusion	45

### **CHAPTER 4            RESULTS AND DISCUSSIONS**

4.1	Introduction	46
4.2	Extraction Region of Interest and Calculation of 3D Images	46
	4.2.1            Two Dimensional Images Information	46

4.3	Assessment of Race from Skull Morphological Features	51
4.3.1	Assessment of Race from Front View Morphological Features	53
4.3.2	Assessment of Race from Side View Morphological Features.	54
4.3.3	Assessment of Race from Bottom View Morphological Features	55
4.4	Comparison of Linear Dimension between Studied Skull and Standard	56
4.5	The Fabrication of Prototype of Normal Asian Human Skull	60
4.6	Capability of Studied Skull Prototype Compare to Previous Study	65
4.7	Conclusion	67

## **CHAPTER 5            CONCLUSION**

5.1	Introduction	74
5.2	Conclusion	74
5.3	Future Recommendations	75

<b>REFERENCES</b>		<b>76</b>
-------------------	--	-----------

## **APPENDICES**

A1	Raw Data CT scans Images	78
A2	Raw Data CT scans Images	79
A3	Raw Data CT scans Images	80
A4	Raw Data CT scans Images	81
A5	Raw Data CT scans Images	82
A6	Raw Data CT scans Images	83
B1	Gantt chart for Final Year Project 1	84
B2	Gantt chart for Final Year Project 2	85

**LIST OF TABLES**

<b>Table No.</b>	<b>Title</b>	<b>Page</b>
4.1	Assessment of Race from Front View Morphological Features	53
4.2	Assessment of Race from Side View Morphological Features	54
4.3	Assessment of Race from Bottom View Morphological Features	55
4.4	Linear Measurement Comparison between Studied Skulls (Present study) and Normal Size Malaysian Skull (Previous Study)	58
4.5	Result of Vibration at Different Height: ABS prototype skull model	67
4.6	Result of Vibration at Different Height: Miraboard 700 prototype Skull model	67
4.7	Material Properties of Skull Prototype and Ball	71

## LIST OF FIGURES

<b>Figure No.</b>	<b>Title</b>	<b>Page</b>
2.1	Posterior view of the skull	6
2.2	View of skull from above	6
2.3	View of skull from lateral position	7
2.4	Various part of human brain	8
2.5	Morphological feature of Caucasoid	9
2.6	Morphological feature of Mongoloid	10
2.7	Morphological feature of Negroid	11
2.8	Different characteristic of different race	12
2.9	A figure to demonstrate rapid prototyping process	13
2.10	Contour detection with grey prediction	16
2.11	Human skull layer-CT data	17
2.12	Skulls and Rapid Prototyping replicas	18
2.13	3D plot of the measured posterior curvatures	19
2.14	Landmarks and reference lines of Skull	20
2.15	Illustration of the size and shape differences between a fossil and a recent skull	22
2.16	Rendered image from MRI data	24
2.17	Images of the completed RP model	24
2.18	Relationship between RP model and FE model	26
2.19	Illustrative representation of the analytical shell model	26
2.20	Silicone gel sample prepared on aluminium cylinders	28
2.21	Development of Brain	29
2.22	Development of initial skull	30
2.23	Development of final version skull	31
2.24	PDMS skin	32

3.1	Flow Chart of Project	34
3.2	2D scan images	36
3.3	All images are loaded and displayed in three views in MIMICS	37
3.4	Rapid Prototyping Machine- 3D Printer	40
3.5	Modeller Machine	41
3.6	Experimental Setup for Drop Ball Test	42
3.7	Sensor cable	43
3.8	Accelerometer	43
3.9	DAQ	44
3.10	Preparing for Skull	45
4.1	A parts of MRI images in DICOM format	47
4.2	3D images calculated from MRI raw data. MRI images are not suitable for extraction process of hard tissues like brain	48
4.3	CT scan raw data of 65 years old female patient	49
4.4	Determination of minimum and maximum value for optimum segmentation	49
4.5	Calculated 3D image in MIMICS software	50
4.6	3D skull models	51
4.7	Skull landmarks for linear measurement	59
4.8	Skull Part in SolidWork drawing	60
4.9	Isometric view	61
4.10	Cutting flow during fabricating of upper part prototype of skull	62
4.11	Cutting flow during fabricating of lower part prototype of skull	63
4.12	The defect that caused by created cutting data error	64
4.13	Complete prototype of skull	65
4.14	Raw data from DASyLab signal process	66
4.15	Vibration versus time at 0.5m height	67
4.16	Height of ball from skull versus vibration	

	(previous study of skull)	68
4.17	Height of ball from skull versus vibration	
	(present study of skull)	68
4.18	Comparison between previous study of skull and present study of skull	69

**LIST OF SYMBOLS**

g	Gravitational acceleration
s	seconds
E	Young Modulus
$\nu$	Poisson ratio
h	Thickness
R	radius
m	mass



**LIST OF ABBREVIATIONS**

CAD	Computer Aided Design
RP	Rapid Prototyping
2D	Two dimensional
3D	Three dimensional
FEA	Finite Element Analysis
CT	Computed Tomography
MRI	Magnetic Resonance Image
SLA	Stereolitograph
SLS	Selective laser sintering
MIMICS	Materialise's Interactive Medical Image Control System
DICOM	Digital Imaging and Communication in Medicine
DAQ	Data Acquisition
FYP1	Final Year Project 1
FYP 2	Final Year Project 2

## **CHAPTER 1**

### **INTRODUCTION**

#### **1.1 PROJECT BACKGROUND**

Human head is a very complex structure consisting of numerous objects with various mechanical properties. Three main components of human's head are skull, scalp and brain which have their own role for human's system. Skull which is cover with scalp is skeletal structure of human's head that protect and form a cavity for the brain, where the nervous system is. Nowadays, prototype of human's skull model needed in wide use such as to educate and train physicians, inform patient, support R&D and for surgical planning.

Leonardo da Vinci was the first to model brain structure by injecting molten wax into the ventricle of an oxen brain. Since then, neuron anatomical models have shown utility in neuroscience and medicine in areas such as education, diagnosis, and surgical planning. Currently, classical modeling techniques are being supplanted by modern methods that emphasize three-dimensional anatomical relationships using imaging techniques (Daniel J.Kelley et al., 2007).

The introduction of rapid prototyping technology has allowed three-dimensional models of human's structure such as skull, brain and bones to be available. Rapid prototyping technology was widely used for prototype development of human's structure with accurate features and sizes. One of the best rapid prototyping techniques is stereolithography. Its medical application was first introduced in 1991 at the Clinic for

Maxillofacial Surgery in Vienna (Lindner et al., 1995). The current clinical applications of the SL model are vast and expanding rapidly.

In modern technology, three dimensional reconstructed image derived from computed tomography (CT) data was the best option available for evaluation and treatment of surgical problems in dental surgery and various other specialties. (A.Nizam et al., 2006) Its main uses are for diagnostics and treatment planning in the field of dental surgery, oncologic surgery, reconstructive surgery and craniofacial surgery (Kermer, 1999). Other uses of such models are as in advance dental implantology procedures, documentation of unusual cases, training of junior staffs and students and patients' education via excellent communication between surgeons and patients in the presence of the model (Ramieri *et al.*, 1999).

## **1.2 PROBLEM STATEMENT**

Technology in rapid prototyping was widely used for many bioscience used. Many natural objects such as skeletal parts, fossil bones or cellular structures can be replicate by using rapid prototyping. However, working with rapid prototyping (RP) technologies in the biosciences differs radically from using them in computational aided design(CAD) environments. In CAD, model is planned and conceived entirely on the computer screen, then converted to physical reality. In bioscience applications, the objects already exist physically. Building models of them essentially involves reverse engineering, starting with acquiring data such as a stack of cross-sectional CT images. Prior to building a replica, these highly complex data need extensive preprocessing (Zollikofer C.P.E et al, 1995).

In the field of human and sport engineering, the rapid skull prototype model is used for education and for experimental study. For example, researcher will use skull prototype model for head impact experiment. In order to get most accurate result of the experiment, the skull model must have almost same dimension and properties to the real human skull. This problem can be overcome by rapid prototyping technology. It will produce skull prototype model from reformatted CT or MRI image which directs the

ultraviolet laser beam to draw layer by layer of the desired structure of skull. In this present study, prototype of human skull is focusing on Asian race.

### **1.3 OBJECTIVES OF STUDY**

The objectives of this study are:

- (i) To develop three dimensional prototype of normal Asian human skull.
- (ii) To determine the capability of prototype of normal Asian human skull through drop ball test experiment

### **1.4 SCOPES OF STUDY**

The following scopes of the study are determined in order to achieve the objectives of the project:

- (i) The human's skull model must follow the morphology features of Asian skull.
- (ii) The human's skull model must have standard dimension of normal human.
- (iii) Prototype of skull model will undergoes drop ball test experiment on force plate in order to check its capability.
- (iv) Two different material skull prototype will undergoes drop ball test which are chemical wood skull, the present study and the Acrylonitrile butadiene styrene (ABS) skull, from the previous study
- (v) The experiment between the two different materials skull prototype need to be done in order to determine the capability of the present study skull prototype.
- (vi) In order to validate the drop ball test experiment results, this study will used analytical method.

## 1.5 REPORT ARRANGEMENT

This report is divided into five chapters. The chapter one is the introduction about the project. It includes the brief project, problem statement, project objectives and the scopes of the study.

The chapter two is discussed about literature review. This chapter provided with introduction of the project design strategies and methods. In here, the general methods to build three dimensional human skull models have been discussed. Then it also includes the brief introduction to various methods to determine the accuracy of the skull model, the way to reconstruct skull model by using rapid prototyping and comparison with previous research method.

The chapter three is discussed about methodology of the project. Firstly the design of project study and frame work is studied. Then it moves to the steps before the STL data of skull will undergoes three dimensional printing processes. . In this study, the design of the project will separate into two work flow, which by the end of this project, the results from the two work flow will be comparing.

The chapter four is focusing on preliminary results and discussion. The three dimensional skull drawing is printed. Then followed by drop ball test for capability determination. Both of the existing result will be comparing. The results also have been analyzed.

The chapter five is about the conclusion and recommendations are made based on the results that have gain in the research. This chapter also mentioned about the alternative way to improve the way of creating rapid prototyping human's skull.

## **CHAPTER 2**

### **LITERATURE REVIEW**

#### **2.1 INTRODUCTION**

In this chapter, it basically describes more about the studies on rapid prototyping process of human structures like skull, brain and teeth with different purpose. Human's skull rapid prototyping processes which has been done earlier by other researchers. It also discussed about the method used to check accuracy of the three dimensional rapid prototyping skull models with the real model by using different ways.

#### **2.2 ANATOMY AND MATERIAL PROPERTIES OF HUMAN HEAD**

Human head is a very complex structure with numerous objects that having many mechanical properties (S. G. M. Hossain, 2010). The head consists of a facial area and cranial skull surrounded by the scalp. The main components of head are skull, brain, scalp and cerebrospinal fluid (S. G. M. Hossain, 2010)

##### **2.2.1 The Skull**

The skeletal structure of the head is divided into three major parts: neurocranium (housing of the brain), face and base. Neurocranium is made of eight bones: frontal, two parietal, two occipital, sphenoid and ethmoid ( N. Yoganandan, 2001). The following figures illustrate these bones making up the human skull (A.Halim,2009)

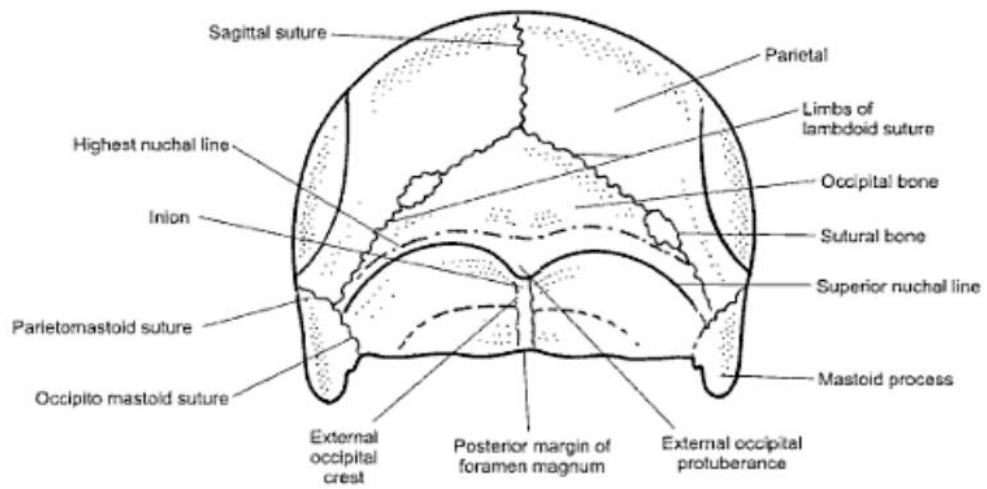


**Figure 2.1:** Posterior view of the skull

Source: A.Halim (2009)

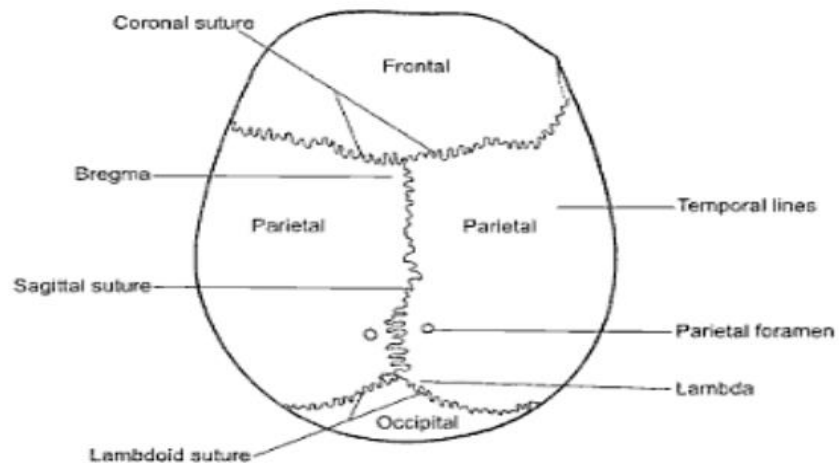


**Figure 2.2:** View of skull from above

Source: A.Halim(2009)

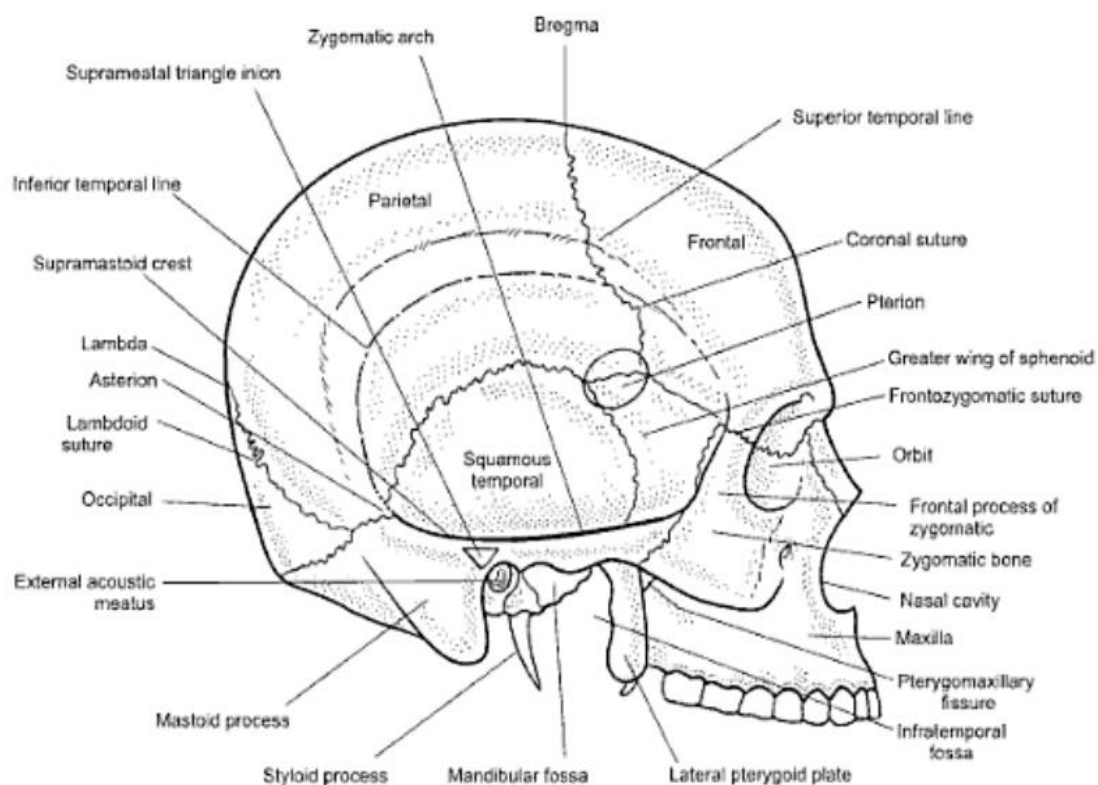


**Figure 2.3:** View of skull from lateral position

Source: A.Halim (2009)

### 2.2.2 The Brain

Human brain is made of mainly two types of cells: neurons and glia. Neurons are the cells that enable the nervous system to carry out all the complex computational functions. A typical human brain weighing 1.3 kg and with a size of 1.5 liters contains an estimated number of 20-100 billion neuron cells. The glial cells are described as the supporting cells for the nervous system; those play an important role of allowing the nervous system to work properly. The estimated number of glial cells in an average human nervous system is 10 times the number of neuron cells (S. G. M. Hossain, 2010)



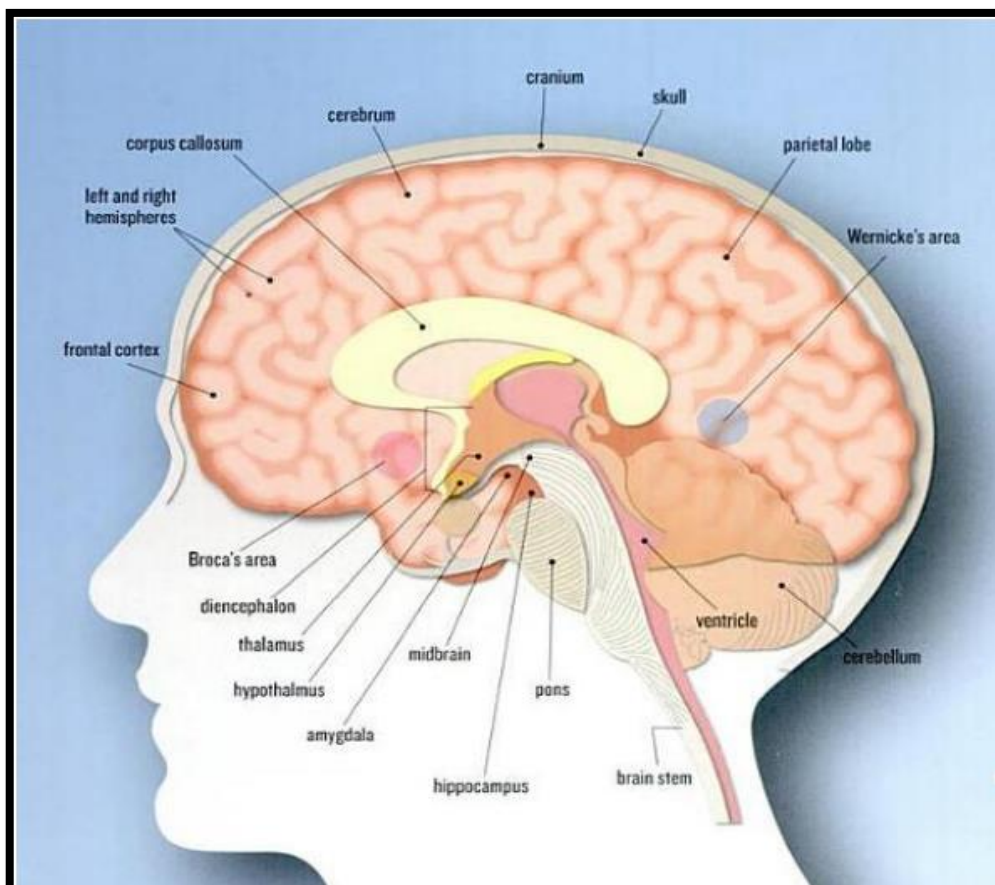


**Figure 2.4:** Various part of human brain

Source: S. G. M. Hossain (2010)

### 2.3 ASSESSMENT OF RACE FROM SKULL

Race concept in the first half of 20th century: so compartmentalized as “species” in the taxonomic sense. (Weidenreich,1947). The dilution during the past century is explicit in the statement “For those of us who were adults in 1950, the old criteria (on race identification) probably still apply. For those born between 1940 and 1970, modifications are probably needed. For those of us born since 1970, the nature and degree of change is mostly unknown, but the probability of change is almost certain” (Hoyme and Iscan ,1989)

### 2.3.1 Determination of Asian Race skull

Over the years, race determination has relied primarily on the morphologic features of the skull and facial skeleton since these provide consistently reliable results in the majority of cases. The three traditional classifications used for race determination are:-

#### a) Caucasoid (White-Europeans, Mediterranean and Americans)

In Whites, this complex includes a high, wide, skull, low cheek, short, gracile zygomatic arches, orthogenetic face, narrow interorbital distance, pointing chin, high nasal bridge, sharp nasal sills, and narrow nasal aperture.

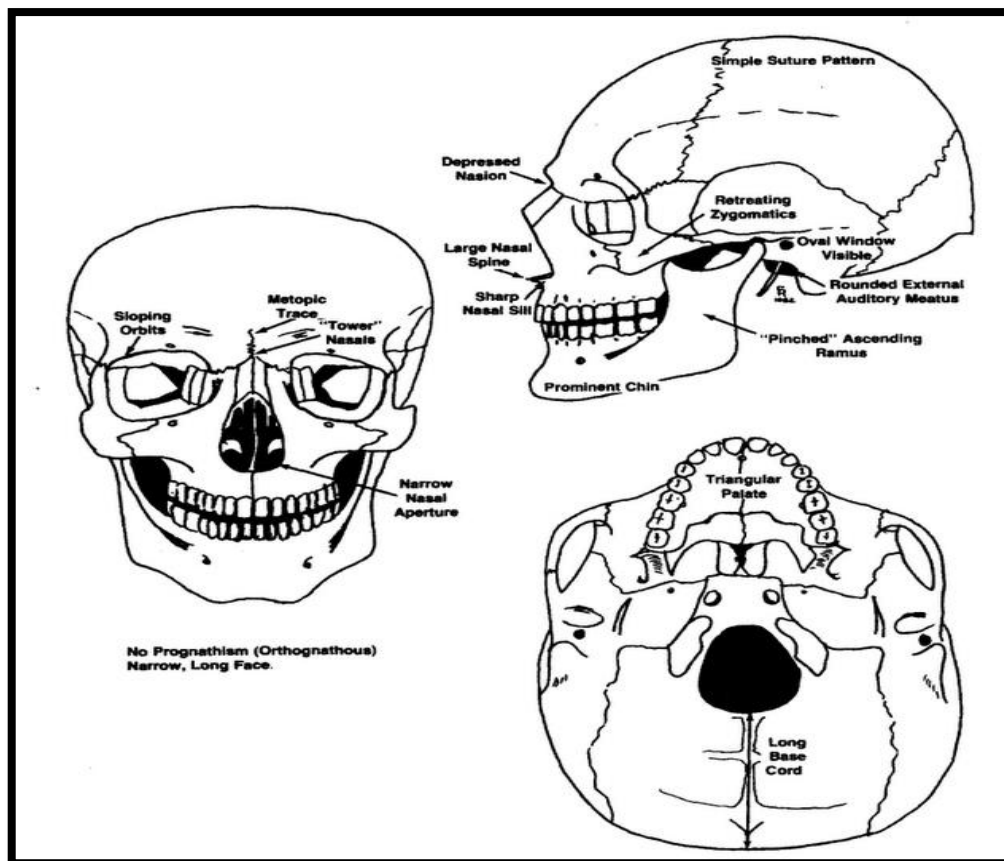


**Figure 2.5:** Morphological feature of Caucasoid

Source : <http://yokeyan-mymind.blogspot.com/2010/12/ill-strain-my-nerves-to-help->

## (b) Mongoloid (East Asian-Asiatic and native Americans)

The Mongoloid complex features a rounder skull, anterior and laterally projecting zygomatic bones, flat face with little projection, shallow nasal root, and shovel-shaped incisors. The most distinctive Mongoloid feature is the cheekbones. They exhibit high malar projection, both anteriorly and laterally, as well as a malar tubercle at the inferior aspect of the zygomaxillary suture. Also, shovel-shaped incisors are much more frequent in Mongoloids.

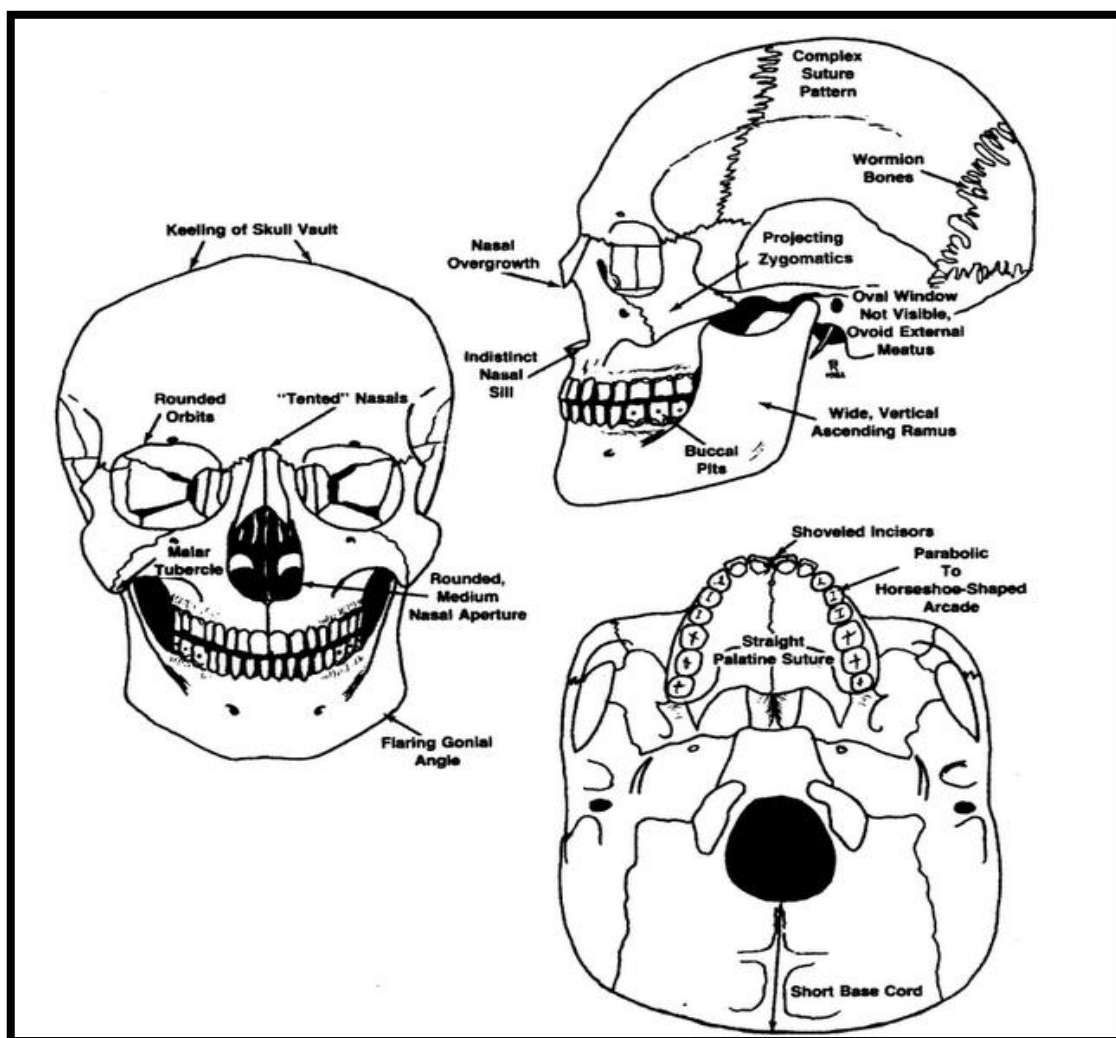
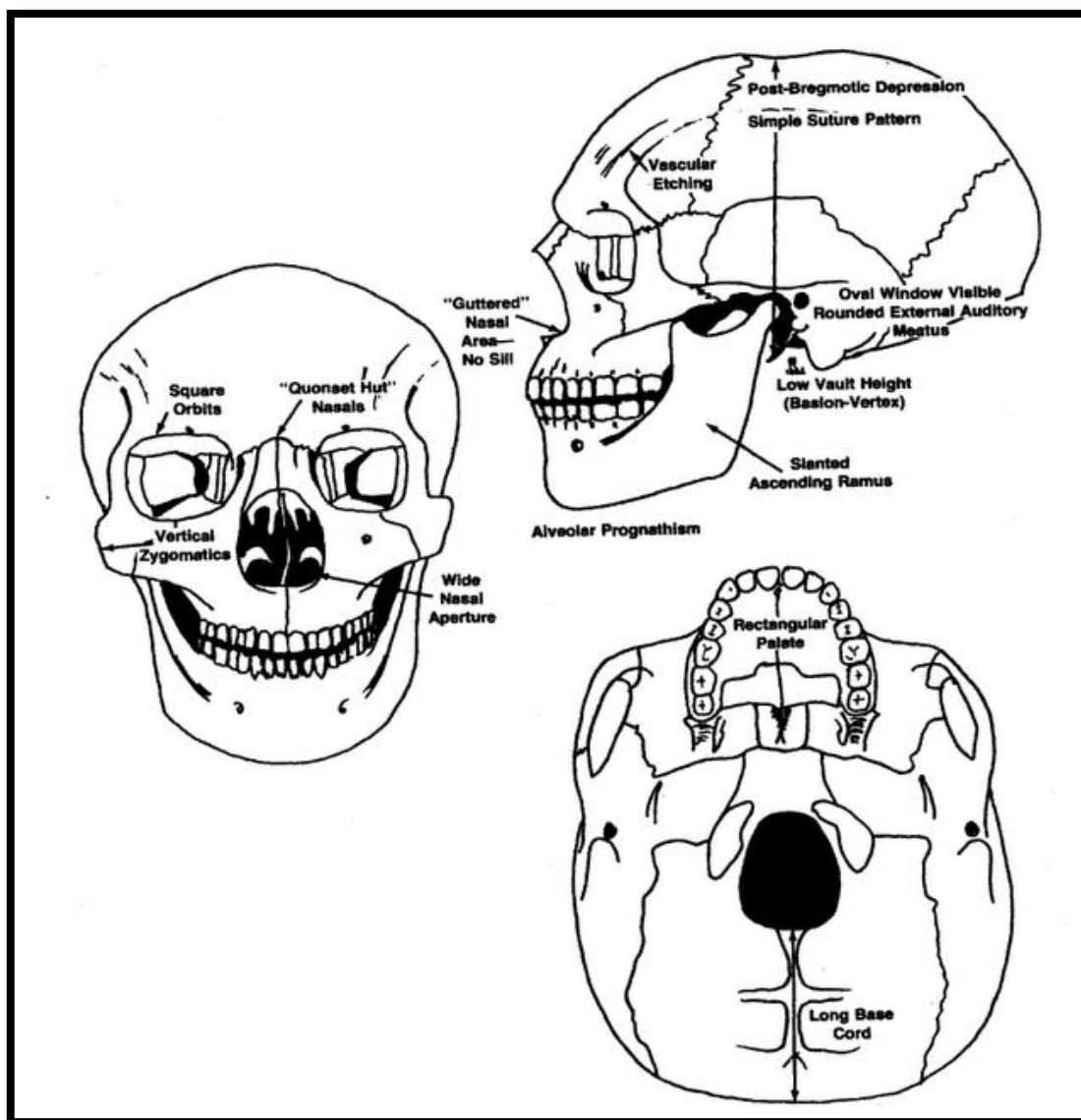


Figure 2.6: Morphological feature of Mongoloid

Source: <http://yokeyan-mymind.blogspot.com/2010/12/ill-strain-my-nerves-to-help->

b) Negroid (Black-Africans and African Americans)

The Black complex is characterized by a long, low, narrow skull, long and robust zygomatic arches that project laterally (relative to the narrowness of the head), alveolar prognathism, wide interorbital distance, receding chin, low nasal bridge, smooth and guttered nasal sills, and wide nasal aperture.



**Figure 2.7:** Morphological feature of Negroid

Source: <http://yokeyan-mymind.blogspot.com/2010/12/ill-strain-my-nerve-to-help->

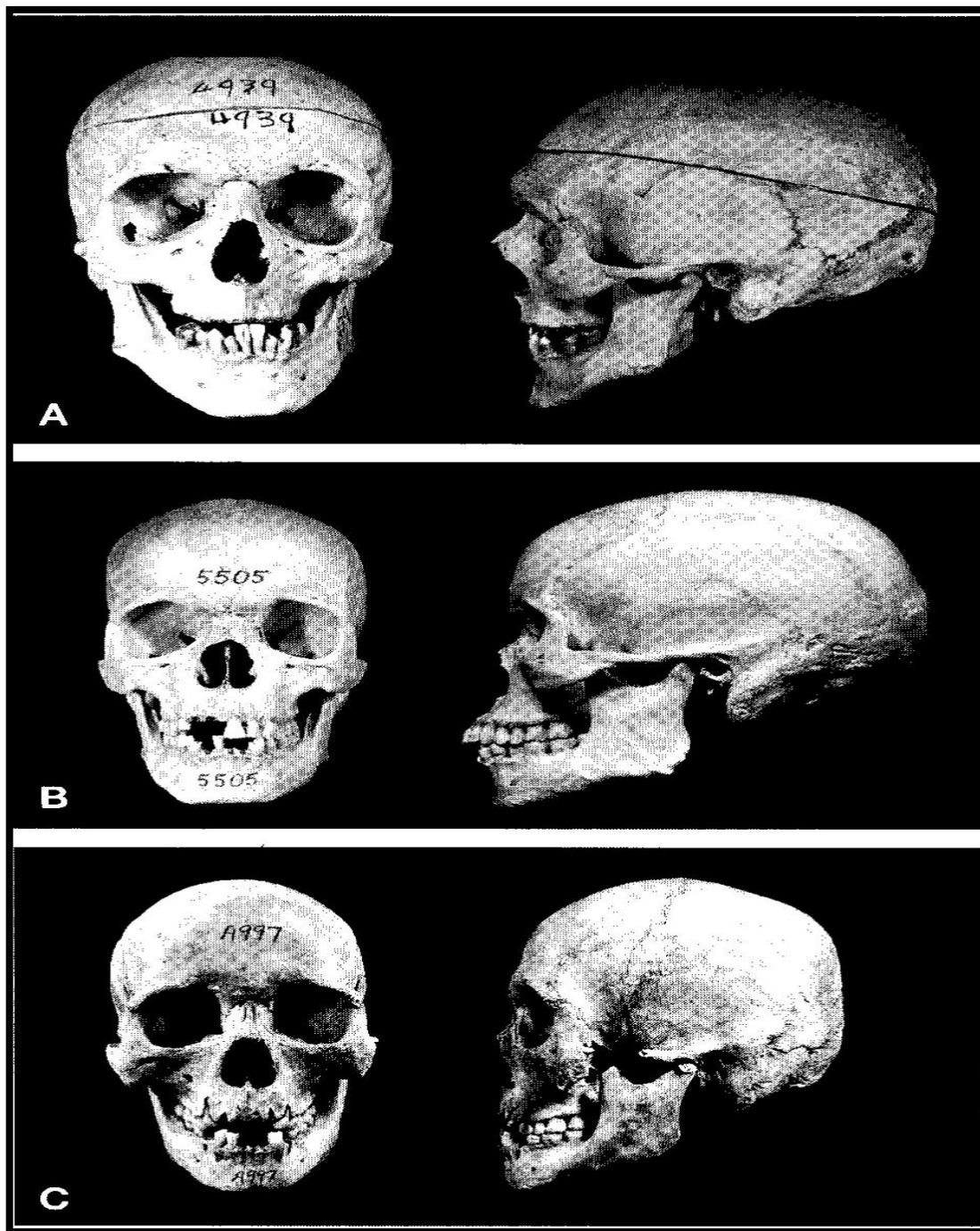


**Figure 2.8:** Different characteristic for different race (a) Caucasoid-Whites tend to have a high, wide head (b) Negroid- blacks often exhibit long, low crania. (c) Mongoloid- Mongoloids are more rounded with flat face

Source: P.T. Jayaprakash (2011)

## 2.4 RAPID PROTOTYPING PROCESS

The rapid prototyping process is a process of converting 3D image in CAD software into three dimensional real models. Basically, stereolithography is a typical modality of rapid prototyping. It produces a three dimensional stereolithography model from reformatted CT images which directs the ultraviolet laser beam to draw layer after layer of the desired structure in a vat filled with a liquid photosensitive resin. These layers of resin, which solidifies upon contact with the laser beam, are superimposed onto each other until the entire model is formed. (A.Nizam, 2006).

Keeping in mind that rapid is a relative term since construction of the model with standard methods requires a few hours to a few days depending on the size and complexity of the model.

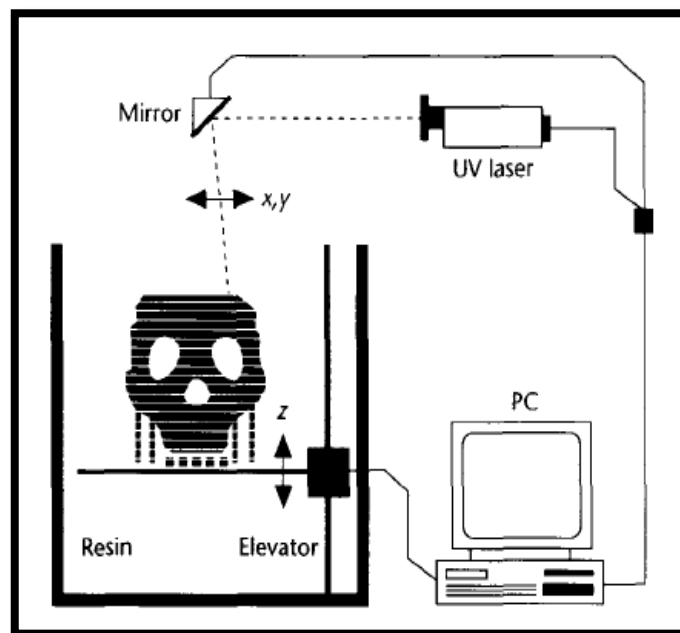


**Figure 2.9:** A figure to demonstrate rapid prototyping process

Source: A.Nizam(2006)

There are a number of types of RP technologies which are:

1. Stereolithography (SLA) uses a vat of liquid resin and a UV laser to build parts that are strong enough to be machined. It is the oldest and most common method of rapid prototyping.
2. Selective laser sintering (SLS) uses a laser to melt (or *sinter*) powders (plastic, metal, ceramic, and glass) into a mass representing the 3D object. SLS claims better accuracy, strength, and stability over time of the models than SLA technologies.
3. Fused deposition modeling uses a plastic filament that supplies material to a nozzle. The nozzle is heated and small beads of thermoplastic form the layers of the object. The material solidifies on contact.
4. Electron beam melting creates metallic objects from metal powder. A layer of powder is placed onto an adjustable surface in a vacuum. An electron beam melts each successive layer of the powder. Unlike SLS and SLA methods, the final product is void-free since the metal is fully melted in each pass. No additional milling step is required.
5. Laminated object manufacturing positions layers of glue-coated plastic, paper, or metal on a platform. A carbon dioxide laser cuts the pattern into the top layer of the material. This process is repeated. No additional manufacturing step is required.
6. 3D printing is the faster and less expensive of the rapid prototyping technologies on the market. A single object can be constructed from multiple materials. 3D printing is optimized for speed, low cost, and ease of use.
7. Stereolithography (SLA) uses a vat of liquid resin and a UV laser to build parts that are strong enough to be machined. It is the oldest and most common method of rapid prototyping.
8. Selective laser sintering (SLS) uses a laser to melt (or *sinter*) powders (plastic, metal, ceramic, and glass) into a mass representing the 3D object. SLS claims

better accuracy, strength, and stability over time of the models than SLA technologies.

9. Fused deposition modelling uses a plastic filament that supplies material to a nozzle. The nozzle is heated and small beads of thermoplastic form the layers of the object. The material solidifies on contact.
10. Electron beam melting creates metallic objects from metal powder. A layer of powder is placed onto an adjustable surface in a vacuum. An electron beam melts each successive layer of the powder. Unlike SLS and SLA methods, the final product is void-free since the metal is fully melted in each pass. No additional milling step is required.

From the previous study, most of the research use stereolithograph technique to build human's skull by using rapid prototyping technology. Laser stereolithograph is an additive process, building objects through layer by layer polymerization of a photosensitive resin. (Zollikofer C.P.E and Leon M.S.P., 1995)

## **2.5 SOURCE OF RAPID PROTOTYPING DATA FOR HUMAN ANATOMY-CT SCAN / MRI IMAGES**

A CT scan stands for Computed Tomography scan. It is a medical imaging method that employs tomography while MRI stands for Magnetic Resonance Imaging, is a test that uses a magnetic field and pulses of radio wave energy to make pictures of organs and structures inside the body. From this raw data, the images are used to render a three dimensional virtual model.

There are many methods that can be applied to reconstruct a 3D solid model for bio-medical imaging from its 2D CT image. The first step in applying this to the recognition of a medical image is to obtain the grey level from the pixel of the image as the value of the prediction series. The steps for image contour detection are threshold value setting, dynamic grey prediction, and image contour detection. The grey level of pixels of the image can be used to carry out dynamic prediction to predict the next point data. The predicted value can then be compared to the actual value from the image. When the difference is greater than the threshold value, the point is recorded as possible



contour point information. After dynamic prediction in the vertical direction is completed, prediction in the horizontal direction is conducted. If both of these predictions suggest that the image data point is a contour point, then it can be assumed that this is the case and that a contour point does exist (Wang C.S, 2009)

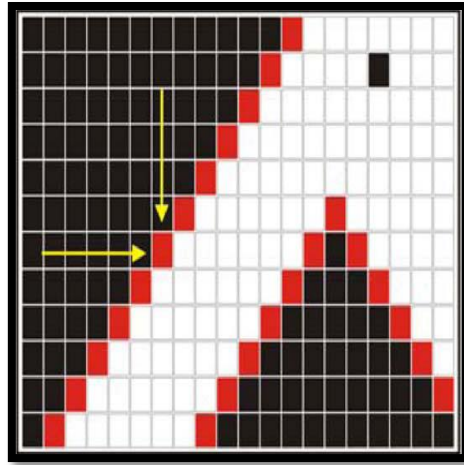


**Figure 2.10:** Contour detection with grey prediction.

Source: Wang C.S (2009)

Usually, this step can be done by using MIMICS software. MIMICS are software used to translate CT data into Rapid Prototyping data. For the present study, MIMICS 8.13 software will be used to edit the raw data from MRI. The resultant 2D image from MRI data was stored in Digital Imaging and Communication in Medicine (DICOM) format before the segmentation of the image was prepared in MIMICS 8.13 software. Finally, the slice files were exported to the RP machine, to produce the replica model of the skull.

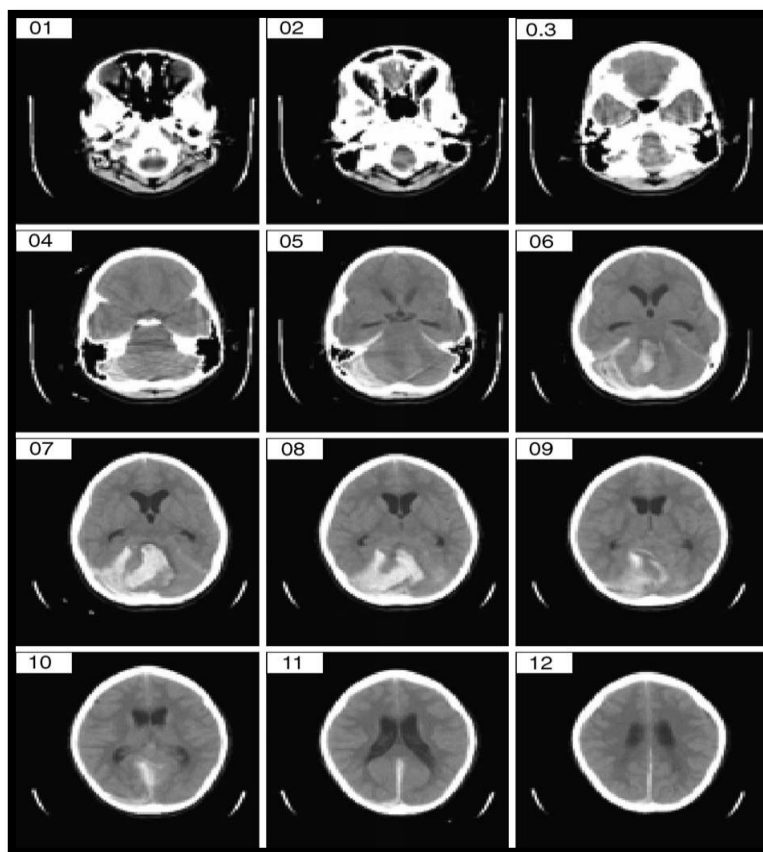


**Figure 2.11:** Human skull layer-CT data

Source: Wang C.S (2009)

## 2.6 ACCURACY OF RAPID PROTOTYPING SKULL MODEL

Many authors have reported regarding the superiority of the SL model for medical applications. Klein *et al.* 1992 reported that accuracy was found to be much higher using the stereolithography system than in milled models. The SL model is also claimed to be able to accurately replicate the surface curvatures of a skull. (Van Lierde *et al.*, 2002). Barker *et al.* (1994) conducted a study to determine the accuracy of producing an SL model by measuring several distance measurements of a dry skull and a geometric phantom and comparing the distance measurement between the anatomical landmarks of both. They reported that the results for the geometric phantom demonstrated a mean difference of +0.47 mm, representing an accuracy of 97.7- 99.1%.

Measurements of the skull produced a range of absolute differences (maximum +4.62 mm, minimum +0.1 mm, mean +0.85 mm).



**Figure 2.12:** Skulls and Rapid Prototyping replicas

Source: Van Lierde et al., (2002)

Many factors are implicated in the dimensional accuracy of the rapid prototyping skull model. The most important determinants of accuracy are the nature of the anatomical region of interest (ROI). Usually, this will occur during image segmentation. The CT scan data that do not captured well by CT scanner will encounter problem because it will had no enough data. This will enable segmentation software to process and convert it to STL file.

Another factor that may cause error in accuracy of the rapid prototyping skull model is CT scanner. In CT scan, there is a protocol that should be follow in order to determine the thickness of image slices. Thinner slices may provide more data that will finally provide smoother surface of the replica model.

The RP system itself that is used to produce the models does have certain critical aspects that frequently need to be validated for accuracy purpose, of which the most important are the RP laser system and the type of resin material use. Daniel J.Kelley et

al., 2007 state that the superior-inferior dimension during model construction because the model was printed in layers from the inferior to superior direction and the weight of the model caused compression along this dimension.

C. Van Lierde1 et al (2002) conducted a study to determine curvature accuracy of RP model. For the purpose of this investigation a total number of 20 cadaver skulls were evaluated A computer was used to load the images made by the video camera and to calculate a point cloud with automatic reconstruction algorithms implemented in the Formetric software.

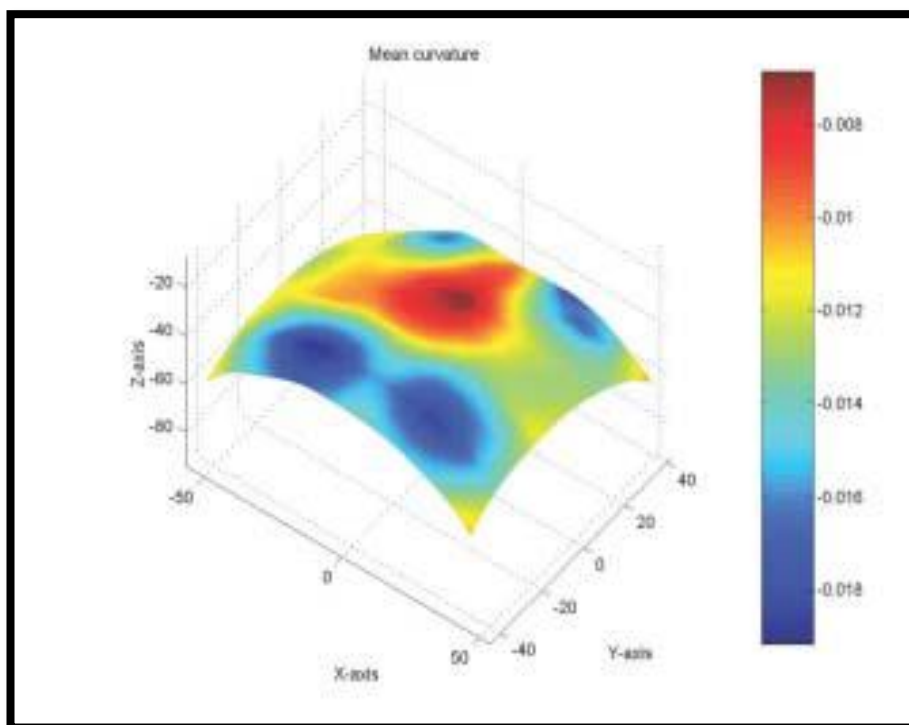


**Figure 2.13:** 3D plot of the measured posterior curvatures

Source: C. Van Lierde1 et al (2002)

## 2.7 LANDMARKS OF SKULL FOR LINEAR MEASUREMENT GUIDELINES

Anatomical landmarks are standard reference points in the face and head used by scientists and physicians. Landmarks tend to be somewhat more abstract than other features of the skull such as protuberances or lines. Skull landmarks are defined by the intersection of sutures, as the extreme points on the skull. These references are relevant to physical measurements and for understanding how appearances change, either slowly, as with aging, or rapidly, as with muscular action.

J.Velemínska, J.Bruzek, P.Velemínský, L.Bigoni, A.Sefčáková and S.Katina (2007) in the journal titled “Variability of the Upper Paleolithic skulls from Czech Republic: Craniometric comparison with recent human standards” study about the diachronic variability in the size and shape of the skull within the territory of Central Europe since the Upper Paleolithic until today.

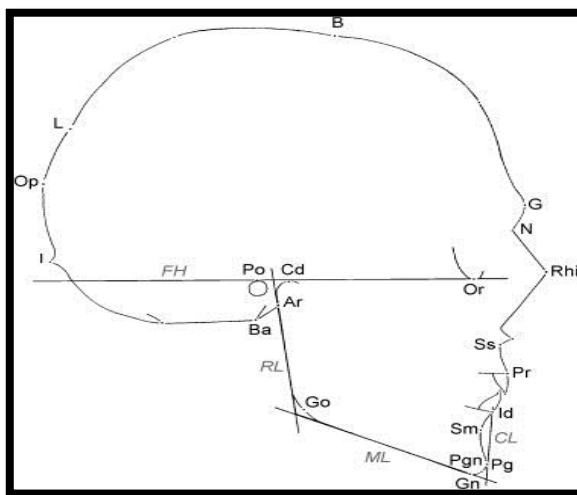


**Figure 2.14:** Landmarks and reference lines of Skull

Source: J.Velemínska(2008)

In this study, the glass negatives of fossil skulls were digitized using special software. Twenty x, y coordinates of key craniometric landmarks were obtained by using SigmaScn Software. The study is based on the comparison of dimensions acquired by different techniques which are measurement of photographs and radiographs.

Landmarks and reference lines used in this study are:-

- |                        |  |
|------------------------|--|
| (a) Ar(articulare)     | : intersection of inferior contour of the posterior cranial base and posterior contour of the ramus. |
| (b) B(bregma)          | : intersection of the coronal and sagittal sutures   |
| (c) Ba(basion)         | : most posteroinferior point on the clivus   |
| (d) Cd(condylion)      | : most superior point on the condylar head   |
| (e) G(glabella)        | : the most anterior point on the arcus superciliaris   |
| (f) Gn(gnathion)       | : the lowest point of the mandibular symphysis   |
| (g) Go (gonion)        | : point on the angle of the mandible determined by the axis of ML/RL angle                           |
| (h) I (inion)          | : top of the protuberantia occipitalis externa   |
| (i) Id (infradentale)  | : point of the alveolar contact with the lower central incisor                                       |
| (j) L (lambda)         | : intersection of the sagittal and lambda sutures  |
| (k) N (nasion)         | : the most anterior point on the frontonasal suture  |
| (l) Op (opistocranion) | : point on the surface of the cranial vault farthest from the glabella point                         |
| (m) Or (orbitale)      | : the lowest point on the orbital margin   |
| (n) Pg (pogonion)      | : the most anterior point on the bony chin   |
| (o) Pgn (prognathion)  | : point on the mandibular symphysis farthest from Cd   |
| (p) Po (porion)        | : the most superior point on the porus acusticus externus  |
| (q) Pr (prosthion)     | : point of alveolar contact with the upper central incisor   |
| (r) Rhi (rhinion)      | : the most anteroinferior point on the nasal bone  |
| (s) Sm (supramentale)  | : the deepest point on the anterior contour of the mandibular symphysis                              |
| (t) Ss (subspinale)    | : the deepest point of the subspinal concavity   |

- (u) CL : the line through Pg and Id
- (v) FH : the line through Or and Po points
- (w) ML : tangent to the mandibular body through Gn
- (x) RL : tangent to the mandibular ramus through Ar



**Figure 2.15:** Illustration of the size and shape differences between a fossil and a recent skull

Source: J.Veleminska(2008)

The size and dimension of fossil and recent skull was compared according to the landmarks points. Mean and standard deviation of three ties reading was calculated and analysed.

## **2.8 PREVIOUS RESEARCH OF PROTOTYPE SKULL/HEAD DEVELOPMENT**

### **2.8.1 On the use of a patient-specific rapid-prototyped model to simulate the response of the human head to impact and comparison with analytical and finite element models, E.A.C. Johnson and P.G.Young (2005)**

E.A.C. Johnson and P.G.Young(2005) in the journal titled “On the use of a patient-specific rapid-prototyped model to simulate the response of the human head to impact and comparison with analytical and finite element models” study about the three way validation of study head injury mechanisms which can broadly be classified as either experimental, analytical or numerical.

MRI data from a young adult male was obtained and rapid prototyped (RP) skull and FE models were generated based on the data. Low velocity impact simulations were performed on both the numerical and experimental models and results are compared with the predictions from the analytical impact model. In previous work (Young, 2003) it has been shown that impacts with low velocity masses are of shorter duration and that short duration impacts could lead to the onset of large, and potentially deleterious, dynamic pressure and shear strain transients in the brain.

For prototype development, MRI image was used and belong to young adult male. The scan was taken axially from the top of the head to the base of the skull. The in-plane coronal slice resolution was 0.9375 mm×0.9375 mm and slice to slice separation was 1.5 mm. The original 3D data set was re-sampled to obtain a 1.5 mm×1.5 mm×1.5 mm cubic volume data set and both manual and semi-automated segmentation was then performed using special software to segment out the skull.



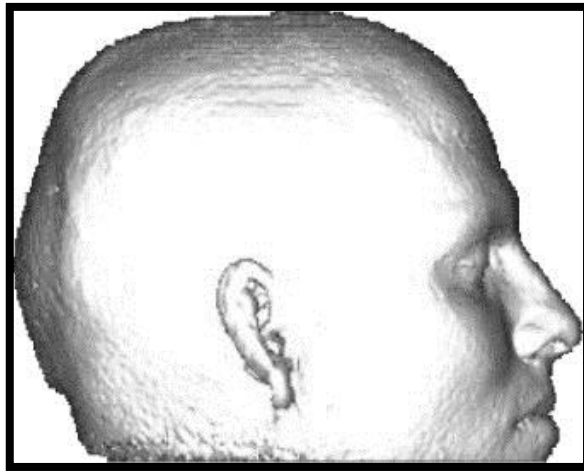


**Figure 2.16** : Rendered image from MRI data

Source: J.Veleminska(2008)

The 3D segmented skull data set was imported into smooth STL format file was generated automatically and used to manufacture a RP model of the skull on a DTM laser sinter station. The material selected for the model was Polyamide(PA) which is typically used when a strong functional prototype is required for testing and evaluation. The Young's modulus of PA as provided by the manufacturer is  $1.6 \times 10^9 \text{ N/m}^2$ . Additionally, PA has a low water absorption value which is an important factor as the RP skull was filled with water in order to represent the brain.

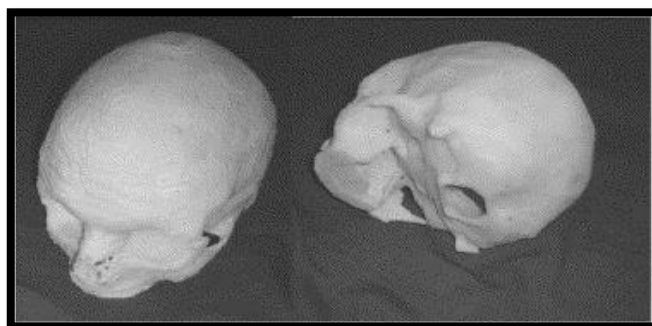


**Figure 2.17** : Images of the completed RP model

Source: J.Veleminska(2008)

The RP skull varies greatly in thickness from 3.70 mm at the most superior part of the parietal bone to 12.62 mm at the base of the occipital bone. Twenty six measurements taken around the skull reveal an average 7.38 mm thickness with a standard deviation of 2.04 mm. The skull also incorporates facial features such as the palate bone which, in this case, averages 1.5 mm in thickness.

The main design of the experimental test rig was based on a pendulum swing system which consisted of an aluminium frame from which a steel impactor was horizontally suspended with fishing wire. The skull was filled with water up to the foramen magnum, this being the most suitable and readily available fluid for replicating pressure wave propagation effects in the brain. The RP skull was either placed inverted on a foam bed for support or held in a cradle suspended from the ceiling

The impactor was made from an 18 mm diameter spherical steel ball halved and pressed onto a shaft, onto which a range of masses could be added. The relative impact velocity was varied straightforwardly by lifting the impactor to a pre-determined height and allowing it to fall freely due to gravity to the base of the swing where the impact occurred. A Kistler 8704B piezoelectric accelerometer, attached to the impactor, was used to measure the acceleration during impact. The peak force transmitted was calculated straightforwardly from the peak acceleration measured by the accelerometer assuming a quasi-static global impact response and using Newton's second law of motion.

In previous work (Young, 2003) an analytical model was proposed to model the impact of a fluid-filled spherical shell of mass ( $m_{sh}$ ), thickness ( $h$ ) and outer radius ( $R_{sh}$ ) with a solid homogeneous isotropic elastic sphere of mass ( $m_{sol}$ ) and outer radius ( $R_{sol}$ ) at a relative velocity ( $\Delta v$ ). The shell was assumed to be filled with an inviscid fluid of density ( $\rho_f$ ) and Bulk modulus ( $B$ ).

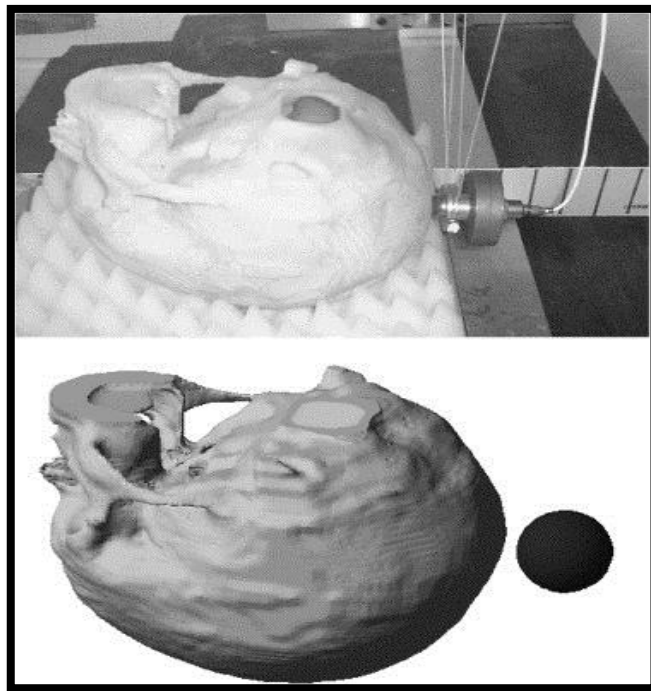


**Figure 2.18** : Relationship between RP model and FE model

Source: J.Veleminska(2008)

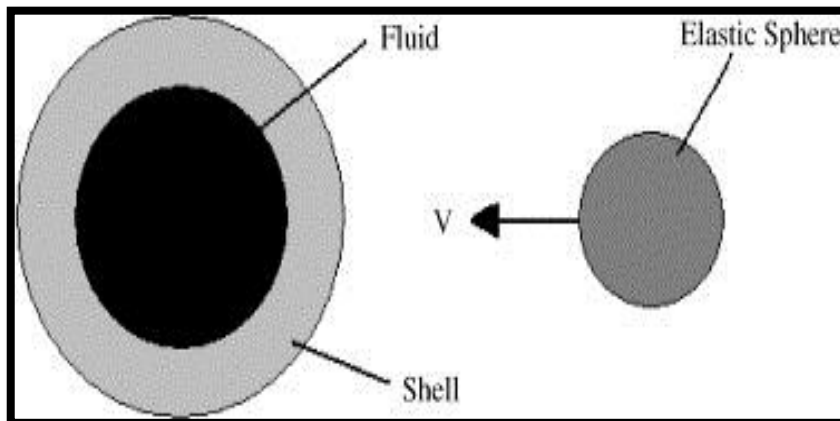


**Figure 2.19**: Illustrative representation of the analytical shell model

Source: J.Veleminska(2008)

Although an implicit expression for  $F_{\max}$  was derived (Young, 2003) from which the impact characteristics can straightforwardly be solved, by introducing further approximations into the model explicit expressions for the impact characteristics were obtained as given here

$$F_{\max} = \frac{R *_{5}^1 E *_{5}^2 m *_{5}^3 \Delta v_5^6 Esh_2^1 h}{\left(\frac{1}{\sqrt{2.3}}\right) R *_{5}^1 E *_{5}^2 m *_{10}^1 \Delta v_5^1 Rsh_2^1 (1 - vsh^2)_4^1 + \left(\sqrt{\frac{3}{2}}\right) \left(\frac{16}{15}\right)_{10}^1 Esh_2^1 h}$$

Where

$$\frac{1}{R *} = \frac{1}{Rsh} + \frac{1}{Rsol}$$

$$\frac{1}{m *} = \frac{1}{msh} + \frac{1}{msol}$$

$$\frac{1}{E *} = \frac{1 - vsh^2}{Esh} + \frac{1 - vsol^2}{Esol}$$

The journal can conclude that analytical, numerical and experimental models were used in parallel to explore the low velocity impact response of the human head. The patient-specific, experimental and numerical models used were generated semi-automatically based on an MRI data set obtained in vivo. Remarkable agreement was achieved between the results obtained from these approaches, providing a three-way validation of these findings.

### 2.8.2 Material Modeling and Analysis for the Development of a Realistic Blast Headform, S. G. M. Hossain (2010)

S.G.M. Hossain(2010) in the journal titled “Material Modeling and Analysis for the Development of a Realistic Blast Headform” study about the blast headform development offers immense importance in the field of traumatic brain injury. Many of these headforms were made for testing impact responses. Among the very few research works focused on blast loading, not all performed rigorous research to simulate brain, skin and skull materials properties and their geometry

Testing and research had been made in order to find out the most suitable materials to replicate human brains, skulls and skins. In this study, the researcher was come out with the result of silicone gel is the most suitable material, which has same properties as real human brain.

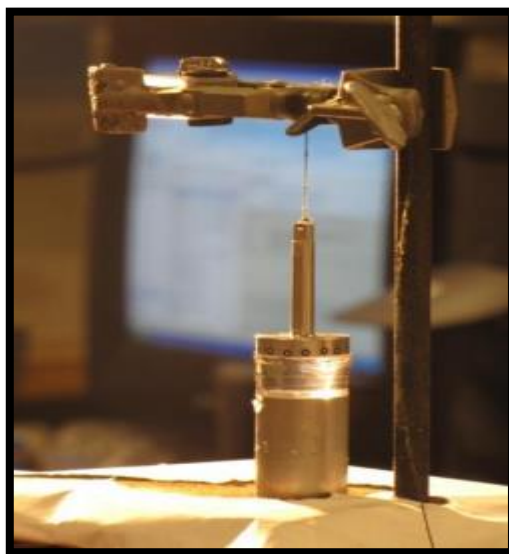
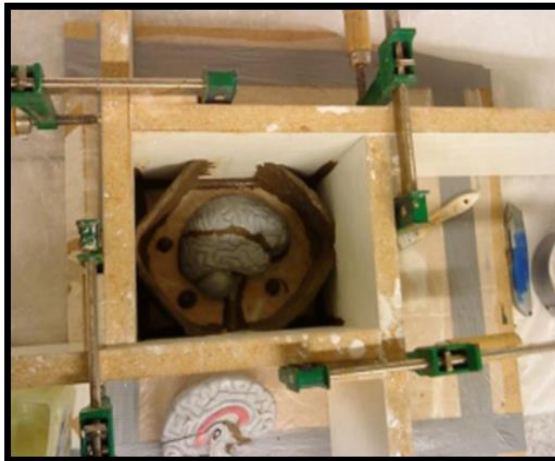


**Figure 2.20** : Silicone gel sample prepared on aluminium cylinders.

Source: S.G.M. Hussain,(2010)

For this experiment procedure, high speed camera was used in order to determine displacement of the silicone gel. To determine its material properties, the

plotted graph from the experiment of determination of displacement of silicone gel versus time was compared to human brain properties. Then, the human brain prototype was developed.



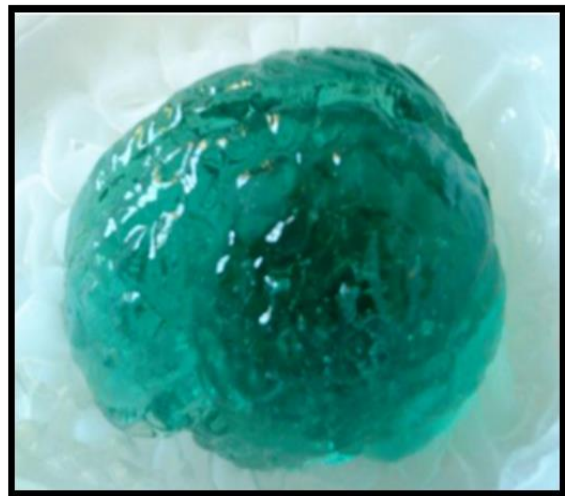
(a)



(b)



(c)



(d)

**Figure 2.21** : Development of Brain (a) Preparation for brain mold; (b) the completed brain mold in a position to pour in gel solution; (c) two parts of brain mold; (d) silicone gel brain

Source: S.G.M. Hussain( 2010)

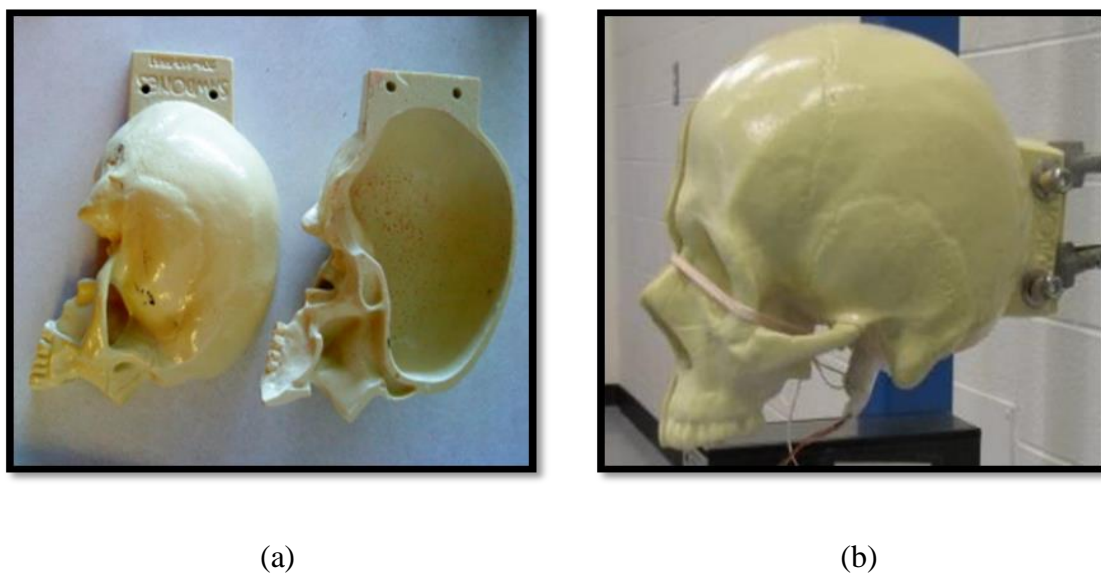


**Figure 2.22:** Development of initial skull (a) Two piece dense foam skull; (b) skull with bolts and clamp attached at the back

Source: S.G.M. Hussain,(2010)

The figure shows the initial model of the skull which has clamp by using bolts. This skull model has geometry alike a real human skull. However, the material properties of this headform were not achieving the properties of actual human skull. Therefore, the researcher needs to find out another method and another material that suit the real human skull properties.

The figure show the final version of the skull which made up of polyurethane. The final version of the skull consists of a mold polyurethane one piece skull. This skull was not as detailed as the previous version in its geometry, but it was expected to have better material properties, being one piece skull, it could offer more consistency in the propagation of shock waves though it into the brain model. This skull had a stainless steel base plate which could be bolted into the bottom of the skull. The plate contained silicone rubber gasket to offer resistance against fluid leakage. This is an advantage, as now it would be possible to insert cerebrospinal fluid simulant inside to offer the head model with more similarity to a real human head. Another feature of the base plate was

that it could be connected to a flexible neck structure which is generally used for crash test dummies. Incorporation of such a neck structure would give the head a flexible movement in front of shock wave.

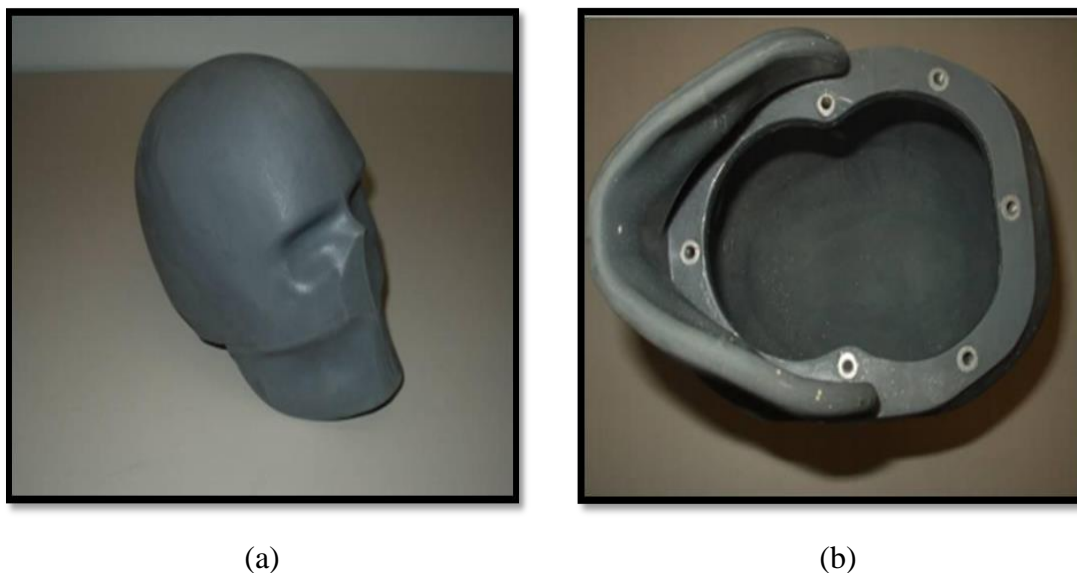


**Figure 2.23:** Development of final version skull (a) One piece polyurethane skull; (b) bottom view of the skull

Source: S.G.M. Hussain,(2010)

For the skin development, the initial head model did not have any skin, but the final one had a two piece skin made of polydimethylsiloxane(PDMS), a silicon based organic polymer. The larger part of the skin covered the cranium, face and neck, and it was attachable over the final version skull. The smaller part of the skin was glued at the back of the skull covering mostly the occipital bone area.

This type of human head development is important in order to come out with most accurate result of experiment. Each part of the human head which are the human skull, human brain and skin need to have same geometry features and same material properties as real human. This type of skull which usually used as dummy for road safety research need to be develop to prevent any risk to the vehicles users and to ensure their safety.



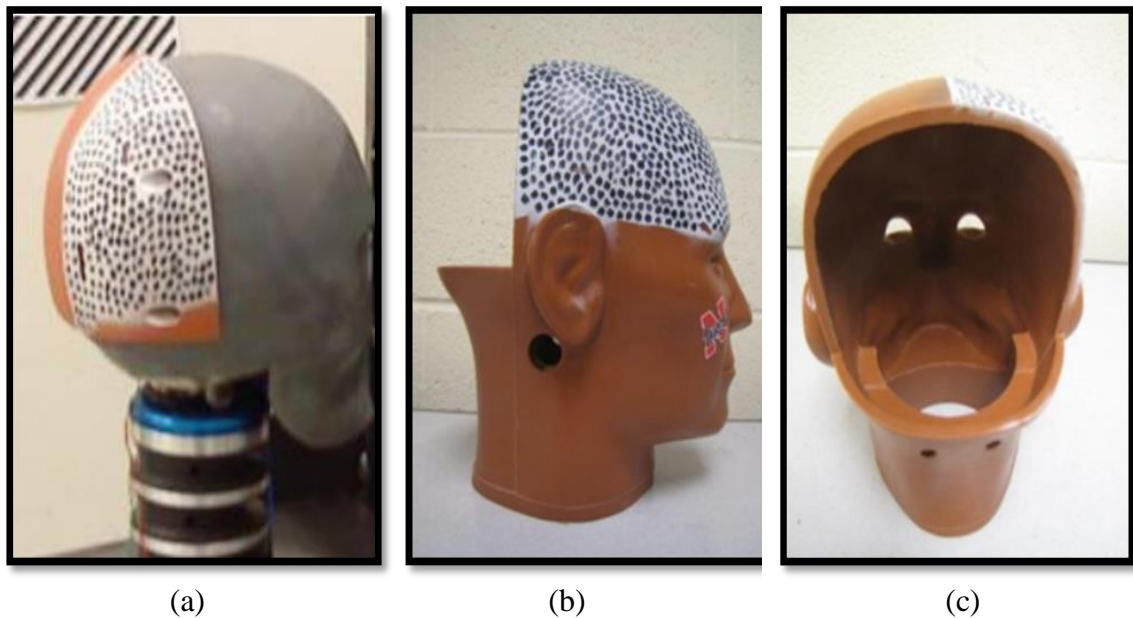


**Figure 2.24:** PDMS skin (a) Part of the skin attached to the skull; (b) the main part of the skin; (c)top back perspective

Source: S.G.M. Hussain,(2010)

## 2.7 SUMMARY

In a conclusion, the technology of rapid prototyping development gives many advantages in bioscience field. The reverse engineering and rapid prototyping pathway we developed has medical application in biomodel guided stereolithograph surgery, cranioplasty, aneurysm research and repair and craniofacial reconstruction. (Kelley D.J et al, 2007). However, the purpose of this study is to create Asian human's skull that can be used in laboratory and class that can be used for learning session.

## **CHAPTER 3**

### **METHODOLOGY**

#### **3.1 INTRODUCTION**

This chapter will explain details of the process on developing of normal Asian human skull prototype. Flowchart system detailing the task need to complete was drafted out. This flow chart shows the overall flow of project in step by step process. There must have a triangular in the flowchart, means that the result obtains from the experiment can be changed if the result is fail. Due to that, the experimental procedures need to conduct again until the expected result is achieved.

The design of the project is a main task need to consider in this chapter. The project with the CT data that need to be converted into STL file. The STL file data can be used in many modelling software such as ALGOR, ADINA and Solidwork. Through this, the STL data can undergo three dimensional printing processes. In this study, the design of the project will separate into two work flow, which by the end of this project, the results from the two work flow will be comparing. Overall, the Final Year Project 1 starts from chapter one that is introduction to chapter 3 which is a methodology. Final Year Project 1 starts from chapter 1 to chapter 5 which is just early conclusion and recommendation. Then will continue with Final Year Project 2 with full chapter 4 (results and discussion) and chapter 5 (conclusion and recommendations).

### 3.2 FLOW CHART

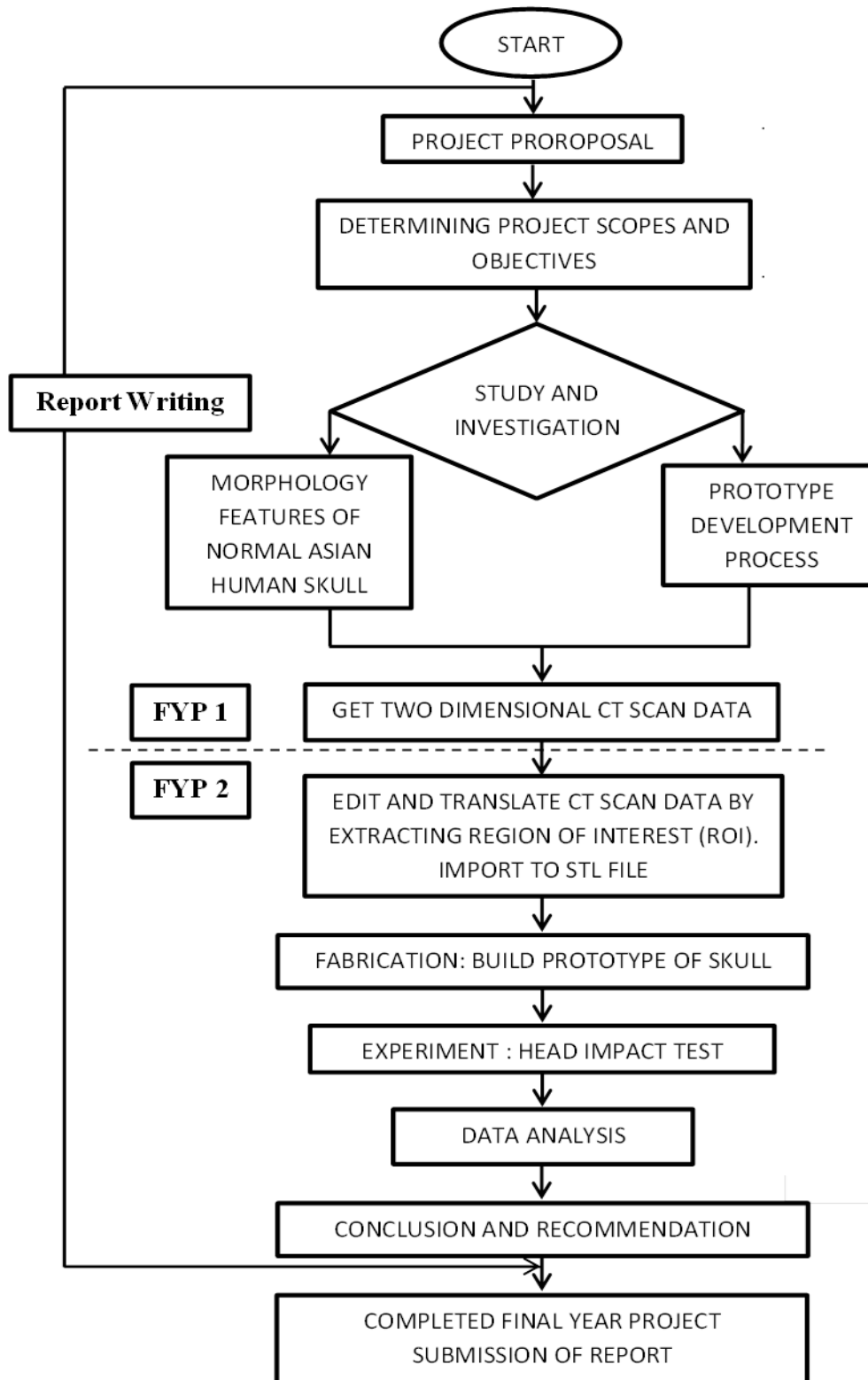


**Figure 3.1:** Flow Chart of Project

### 3.3 DESIGN OF PROJECT STUDY

This project begins with an appointment with the supervisor at the first week study. The title of the Final Year Project is Prototype Development of Normal Asian Human's skull. Then, this project proceeds with a discussion with the proposed supervisor to detail out the project problem statement, project objectives and project scopes. At the same time, weekly appointment with the supervisor is arranged.

The prototype development process of the skull is studied in this project. The study starts by identifying the most basic steps to create three dimensional skull replicas. Also, in order to achieve the scopes of study, morphological features of a normal Asian human skull are sturdy. There are three main skull races and each of them has different features and characteristics. The knowledge about the morphological features of the skull is important in this research so that the recent three dimensional skulls can be determined as Asian skull. Other than that, the standard sizes of the normal skull need to be investigated and determine in order to achieve the scopes of study.

The next stage is to find journal, thesis, books, websites and conference about prototype development of human skull regarding the project title as reference for literature review of the project. Some journals are referred from the university's database such as the journals from previous project that have been done by the senior students. Several journals have been studied and kept as a future reference to be used later. The previous thesis of final year student also referred as a source of information while doing the project. All the collected information will be used as guide to finish the study.

Then, the project flow is designed. The project flow or methodology needs to be designed as a guide for us to complete the project systematically before the due date of the Final Year Project. From the journal and supervisor advice, the way to complete the project can be improved. Besides, the previous research method also included in literature review as guide to do this project.

### 3.4 RAW DATA FROM CT SCAN IMAGES

In order to get accurate normal Asian human's skull, computed tomography (CT) data will be used as raw data before the fabrication process of the skull by using rapid prototyping technology. A CT scan stands for Computed Tomography scan. It is a medical imaging method that employs tomography while MRI stands for Magnetic Resonance Imaging, is a test that uses a magnetic field and pulses of radio wave energy to make pictures of organs and structures inside the body. From this raw data, the images are used to render a three dimensional virtual model.

CT scan images and MRI images which is in two dimensional come out with many layers of image with different thickness and image pixels. The thinner the images, the finer the three dimensional skull models will be create. This factor will influence the accuracy and the product of my study.

Compare to MRI images, CT scan images is more suitable to be used in my study because of its ability to detect hard tissue while MRI images is more suitable to be used in study that is related to soft tissues such as brain, heart kidney and other internal organs. Hard tissues which included all parts of human bone can be seeing clearly in CT images.

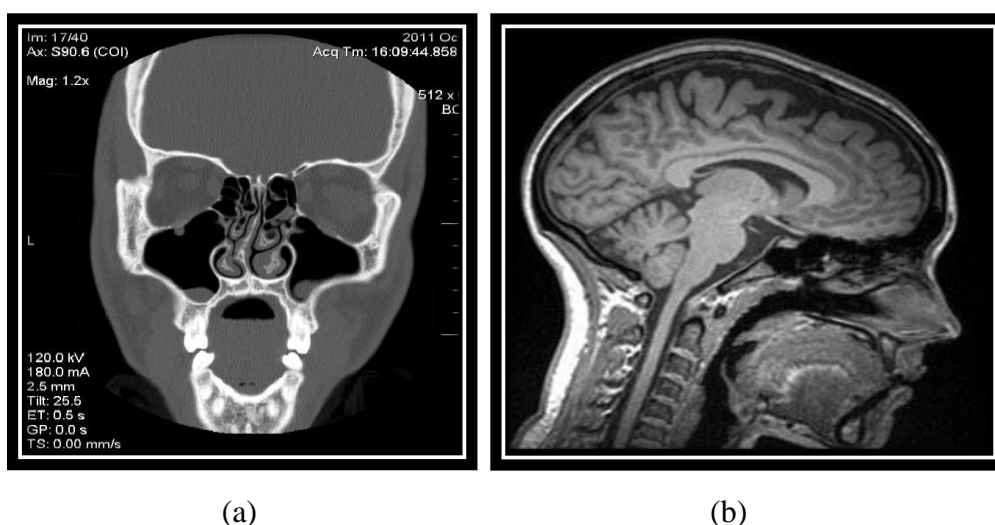


**Figure 3.2:**2D scan image. (a) CT scan image has more intensity of skull (hard tissue)  
(b)MRI image has more intensity of brain (soft tissue)

### 3.5 EXTRACT REGION OF INTEREST PROCESS

The raw data from MRI or CT images was in two dimensions. In order to create a virtual model from this two dimensional raw data, we need to calculate it into three dimensions. Materialise's Interactive Medical Image Control System (MIMICS) are one of the software that can be used to translate CT scan data image into rapid prototyping data. MIMICS are a general-purpose segmentation program for gray value images. It can process any number of 2D image slices.

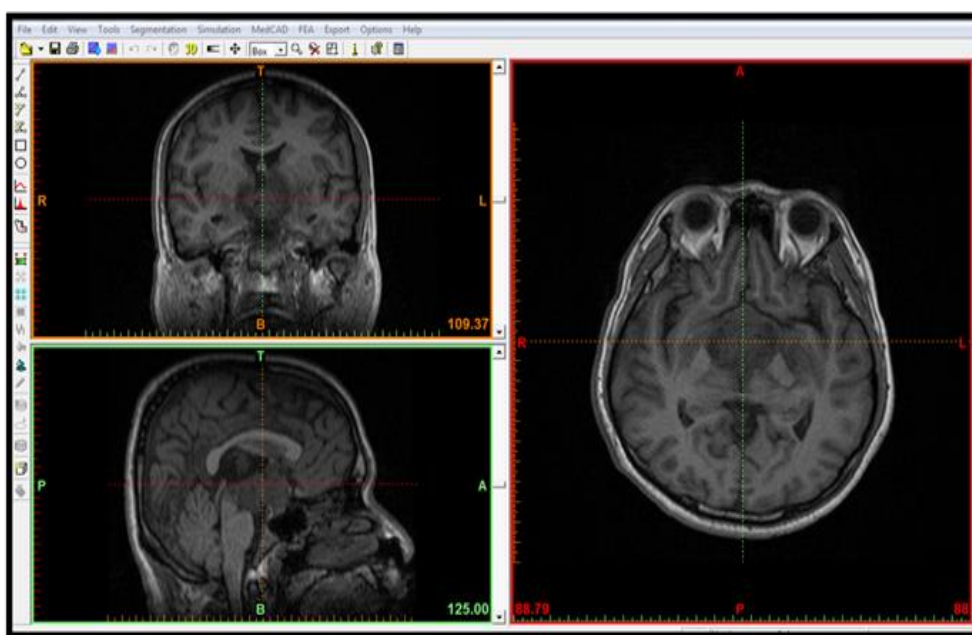


**Figure 3.3:** All images are loaded and displayed in three views in MIMICS

MIMICS are an interactive tool for the visualization and segmentation of CT image. All images are loaded and displayed in three views. The view on the right shows the images as they are exported by the scanner. The upper left corner is a reslice of these images in the xz-direction and the bottom left is a reslice in the yz-direction. The different colors of the intersecting lines refer to the colors of the contour lines of each view so every line refers to the slice in the corresponding view. It can easily navigate through the images by clicking on any point of the CT images in any view: the intersecting lines will move crossing each other in the point you clicked and all the views will be updated showing the corresponding slices. Therefore, in the medical field

MIMICS can be used for diagnostic, operation planning or rehearsal purposes. A very flexible interface to rapid prototyping systems is included for building distinctive segmentation objects.

### **3.6 FABRICATION: PROTOTYPE DEVELOPMENT PROCESS**

Usually, prototype development process will be done by using rapid prototyping machine. Rapid prototyping (RP) technologies construct physical models from virtual designs usually from STL data by successively layering materials such as plastic and metal. Unlike a CNC machine that removes material, RP is an additive process. This type of fabrication is inexpensive for producing small quantities of a model typically for testing fit, form, and function though there are many applications of RP that produce one of a kind objects. The first step in the rapid prototyping process is to create a 3D model of the object that we wish to manufacture from modelling software. There are a number of types of RP technologies which are:

1. Stereolithography (SLA) uses a vat of liquid resin and a UV laser to build parts that are strong enough to be machined. It is the oldest and most common method of rapid prototyping.
2. Selective laser sintering (SLS) uses a laser to melt (or *sinter*) powders (plastic, metal, ceramic, and glass) into a mass representing the 3D object. SLS claims better accuracy, strength, and stability over time of the models than SLA technologies.
3. Fused deposition modeling uses a plastic filament that supplies material to a nozzle. The nozzle is heated and small beads of thermoplastic form the layers of the object. The material solidifies on contact.
4. Electron beam melting creates metallic objects from metal powder. A layer of powder is placed onto an adjustable surface in a vacuum. An electron beam melts each successive layer of the powder. Unlike SLS and SLA methods, the

final product is void-free since the metal is fully melted in each pass. No additional milling step is required.

5. Laminated object manufacturing positions layers of glue-coated plastic, paper, or metal on a platform. A carbon dioxide laser cuts the pattern into the top layer of the material. This process is repeated. No additional manufacturing step is required.
6. 3D printing is the faster and less expensive of the rapid prototyping technologies on the market. A single object can be constructed from multiple materials. 3D printing is optimized for speed, low cost, and ease of use.
7. Stereolithography (SLA) uses a vat of liquid resin and a UV laser to build parts that are strong enough to be machined. It is the oldest and most common method of rapid prototyping.
8. Selective laser sintering (SLS) uses a laser to melt (or *sinter*) powders (plastic, metal, ceramic, and glass) into a mass representing the 3D object. SLS claims better accuracy, strength, and stability over time of the models than SLA technologies.
9. Fused deposition modelling uses a plastic filament that supplies material to a nozzle. The nozzle is heated and small beads of thermoplastic form the layers of the object. The material solidifies on contact.
10. Electron beam melting creates metallic objects from metal powder. A layer of powder is placed onto an adjustable surface in a vacuum. An electron beam melts each successive layer of the powder. Unlike SLS and SLA methods, the final product is void-free since the metal is fully melted in each pass. No additional milling step is required.

From my reading, most of the research use stereolithograph technique to build human's skull by using rapid prototyping technology. Laser stereolithograph is an



additive process, building objects through layer by layer polymerization of a photosensitive resin. (Zollikofer C.P.E and Leon M.S.P., 1995)

In Rapid Prototyping Laboratory of Faculty of Mechanical Engineering, Universiti Malaysia Pahang, there are two options that can be applied to develop the prototype. The first option is powder based rapid prototyping, which an additive process concept. The material used for this machine is powder. This prototype development machine is very suitable to build a model as a preview look for the new products which the created model or prototype has a very low hardness and not suitable to be used or undergo testing experiment.

The second option is modeller machine, which has a subtractive process concept. There are many materials can be process by this machine and the created model may be strong enough for be used and undergo testing experiment. The table below show the comparison between two prototype development machines provided by Rapid Prototyping Laboratory in Faculty of Mechanical Engineering, Universiti Malaysia Pahang.



**Figure 3.4** : Rapid Prototyping Machine- 3D Printer



**Figure 3.5:** Modeller Machine

As the next procedure of the research is to test the 3D skull model, high hardness of skull prototype is needed. Therefore, in this study, the Modeller Machine that able to produce high hardness skull prototype will be used. For Modeller Machine, the STL file skull model will be simulate in SRP software to calculate estimate time for the cutting process and to set up the program for cutting process. Then, the research will be continuing with the head impact test.

### **3.7 EXPERIMENT:DROP BALL TEST**

After fabrication process of skull prototype is done, the next project flow is to determine the capability of normal Asian human skull prototype compare to the previous study. The objective of this experiment is to determine the vibrations that occur in ecogel 200 that has same properties as brain. The ecogel 200 will be located in skull prototype where the brains locate. An experiment was designed in which the balls were dropped at different velocity onto a skull prototype in certain different high. . Dropping from a height also allows the effect of drag forces on the balls. The experiments were conducted indoors to discount the effects of air movement.

### 3.7.1 Experimental Setup for Drop Ball Test

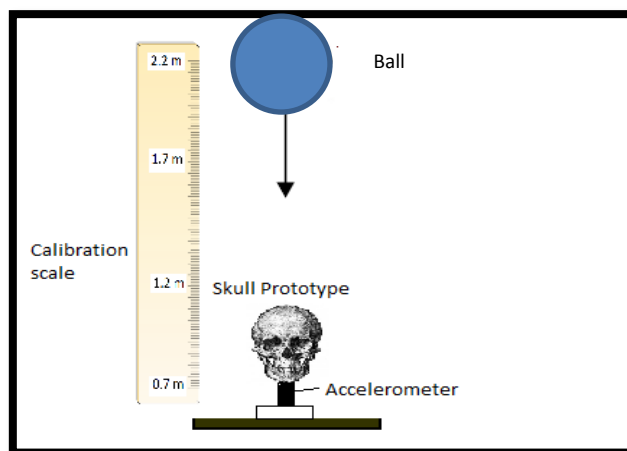


**Figure 3.6:** Experimental Setup for Drop Ball Test

The test will be done at three different heights which are 0.5m, 1.0m and 1.5m. The drop ball will be repeated 3 times for each height in order to get an average reading for each height.

### 3.7.2 Equipment used for experiment

Tri-axial accelerometer, data acquisition (DAQ) device, sensor cable, stopwatch, digital camera and archery target board.

In this experiment, sensor cable will be used to connect the compact DAQ with the sensor. Sensor that been used in this project is the accelerometer. This cable consist of 3 channel that is x, y, and z. Each of the cable will then connected to the DAQ counter located at the bottom. Thus, acceleration now can be signal out into this device to be program as output data.



**Figure 3.7:** Sensor cable

Also, tri-axial accelerometer will be used. An accelerometer is a device that measures proper acceleration. It can detect the acceleration data in 3 axis that are y-axis, x-axis, and z-axis. This accelerometer will be detached at the arm of the subject in order to measure the acceleration data during shooting processes.



**Figure 3.8:** Accelerometer

Data acquisition (DAQ) device used is National Instrument DAQ NI cDAQ-9171. The NI cDAQ-9171 is a bus-powered, 1-slot NI CompactDAQ USB chassis designed for small, portable sensor measurement system. Combine the cDAQ-9171 and one of the over 50 NI C Series measurement-specific modules to create an analog output, digital I/O, or counter/timer measurement system. Modules are available for a

variety of sensor measurements including thermocouples, RTDs, strain gauge, load and pressure transducers, torque cells, accelerometer, flow meters, encoders, and microphones. NI CompaqDAQ system combine sensor measurements with voltage, current and digital signal to create custom measurement systems with a single, simple USB cable back to the PC, laptop or netbook. The cDAQ-9171 has four 32-bit general purpose counter/timer built in.

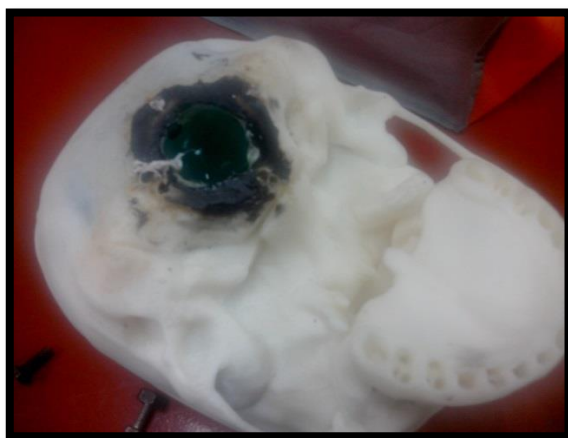


(a)



(b)

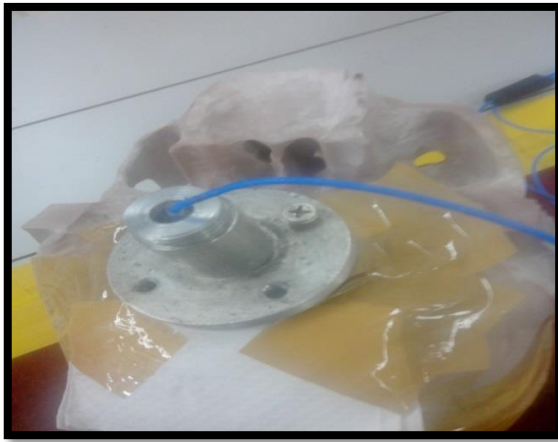
**Figure 3.9:** (a) Front view (b) back view of the cDAQ-9171



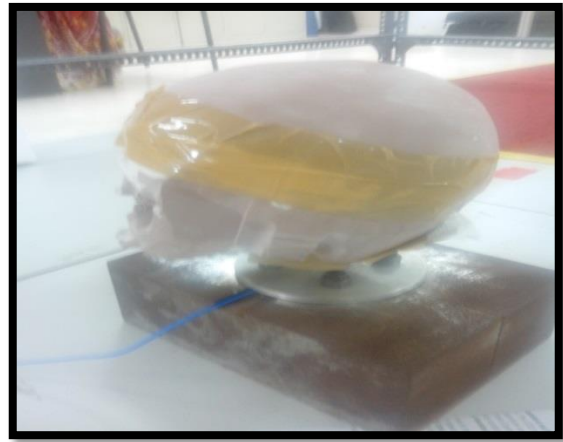
(a)



(b)



(c)



(d)

**Figure 3.10:** Preparing for skull: (a)The skull prototype was inserted with ecogel 200;(b)The accelerometer covered with plastics connected with sensor cable was inserted inside the skull prototype;(c)Then, the skull was ready for experiment;(d)The skull prototype placed on the special block, ready for experiment

## **CHAPTER 4**

### **RESULTS AND DISCUSSIONS**

#### **4.1 INTRODUCTION**

This chapter provide results of this project that are obtained by planned methodology. In this chapter, the discussions about the fabrication process will be briefly explained. As discussed in the previous chapter, after fabrication of skull prototype done, the research was continue with experiment which the skull prototype inserted with jelly will undergoes drop ball test which the vibration of the jelly will be study and analyse in this chapter.

#### **4.2 EXRTACTION REGION OF INTEREST AND CALCULATION OF 3D IMAGES**

##### **4.2.1 Two Dimensional Images Information**

One of the requirements to finish this project is to get raw data of human's head image. From my reading, I have found that these 2D images must be either from MRI or CT scan which this scanner machine will scan patients body resulting a 2D images. Then, the 2D images need to be process in MIMICS software which this MIMICS software was used to extract the needed region from the 2D images before the highlighted region will be converted into 3D images.

At first, I manage to get MRI raw data from government hospital in Malaysia. The data belong to thirty two years old Malaysian's male. The data consists of one hundred and seventy six (176) slices which thickness of each slice is about 15mm. Each slice represent different layer of human's skull. The thickness and the number of the image is important factors that may influence the product of this project where the higher the number of images the finer the surface of the prototype and the lower the thickness of the image, the more accurate features of human skull will be produce.

Then, all the slices of MRI 2D images which are in Digital Imaging and Communication in Medicine (DICOM) format will be export into MIMICS software as discussed in previous chapter. For this research, MIMICS 8.13 version is used and the information about the MIMICS software has been mentioned before in the previous chapter.

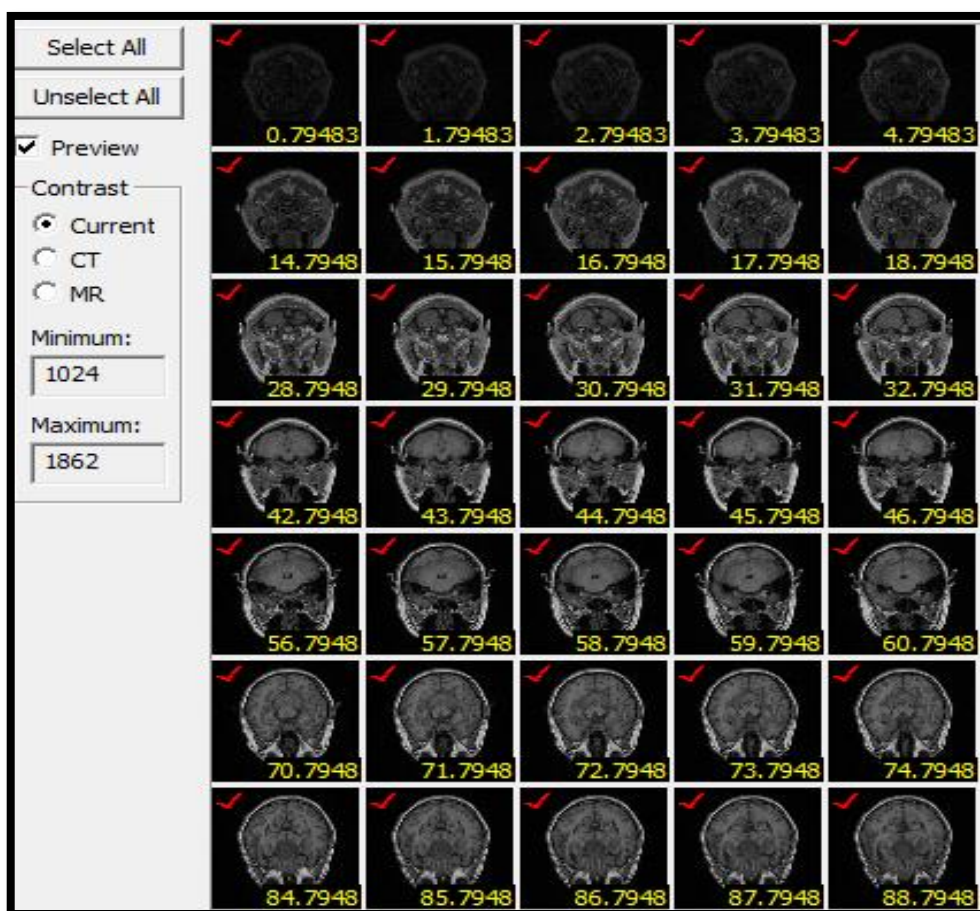


**Figure 4.1:** A parts of MRI images in DICOM format



Unfortunately, when processed in MIMICS software, the skull part from these images cannot be extracted due to MRI image have high intensity of soft tissues. Only soft tissues like brain can extract from MRI images. Differ to CT scan images which have high intensity of hard tissues like skull and bones, this type of 2D images is more suitable for my project.

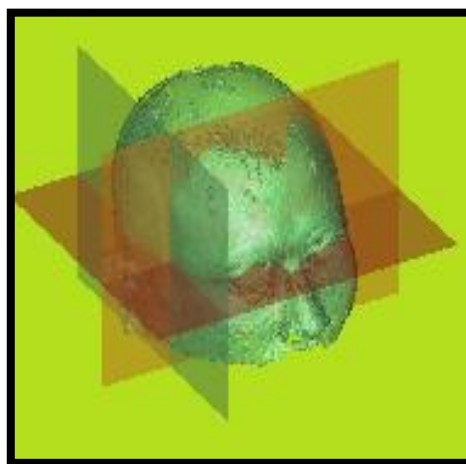


**Figure 4.2:** 3D images calculated from MRI raw data. MRI images are not suitable for extraction process of hard tissues like brain.

Therefore, this research need to be proceeding with another type of raw data images which is 2D CT scan images. Centre of Sport Engineering, Universiti Malaysia Pahang had tried to make collaboration with Hospital Universiti Sains Malaysia for advices, ideas, knowledge and sharing of raw data from the Department of Radiology Hospital Universiti Sains Malaysia. Luckily, the Department of Radiology Hospital Universiti Sains Malaysia agreed to give us CT scan images of human's head for research purpose. This CT scan images was belong to 65 years old female patients which consists of 286 layers of images with 8mm thickness for each.

The two dimensional CT scan images was imported to MIMICS 8.13 software for extraction process. The first step in applying this to the recognition of a medical image is to obtain the grey level from the pixel of the image as the value of the prediction series. The steps for image contour detection are threshold value setting, dynamic grey prediction, and image contour detection.

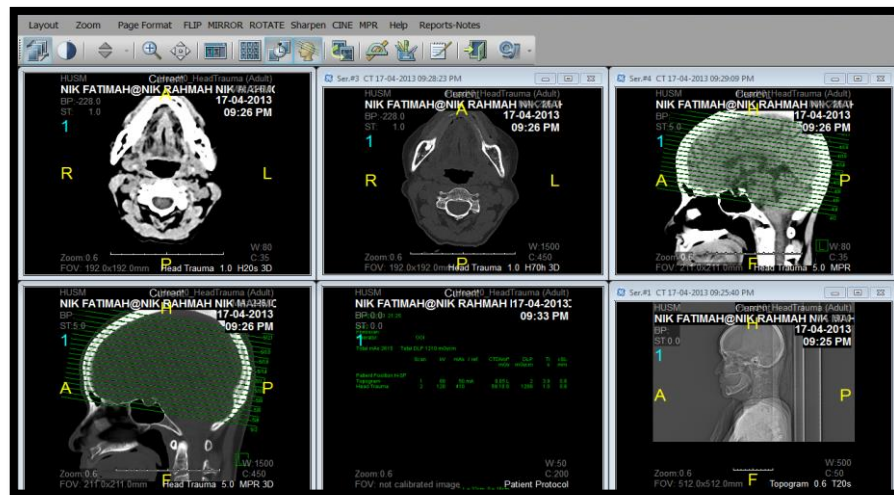


**Figure 4.3:** CT scan raw data of 65 years old female patient

. The grey level of pixels of the image can be used to carry out dynamic prediction to predict the next point data. The predicted value can then be compared to the actual value from the image. When the difference is greater than the threshold value, the point is recorded as possible contour point information. After dynamic prediction in the vertical direction is completed, prediction in the horizontal direction is conducted. If both of these predictions suggest that the image data point is a contour point, then it can be assumed that this is the case and that a contour point does exist (Wang C.S, 2009).

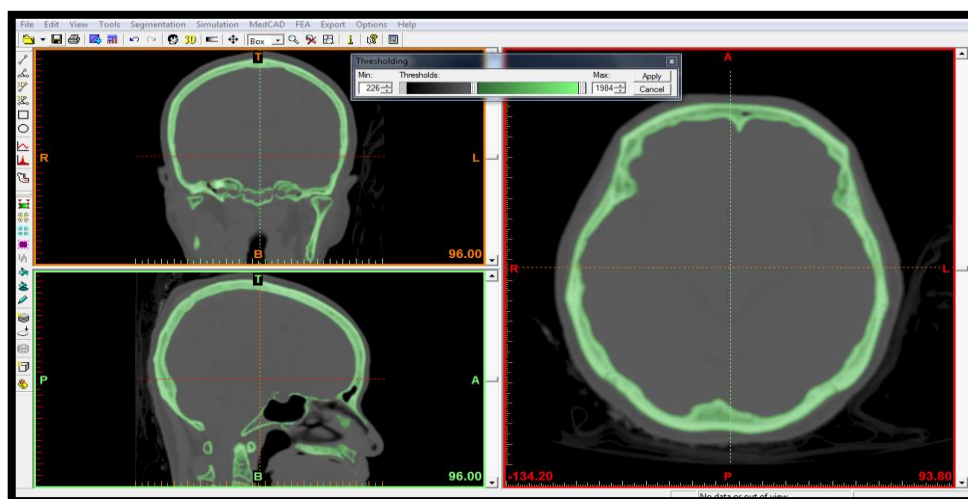


**Figure 4.4:** Determination of minimum and maximum threshold value for optimum segmentation.

The figure shows the procedure of determination threshold value. In this present study, the suitable value for minimum threshold value is 226 while the maximum threshold value is 1984. This procedure is important in order to obtain 3D skull model with complete and smooth hard tissue for the real skull. The threshold value is different for a different organs or tissues needed depending on its density of the tissues. For example, brains which have lower density compare to skull may have different minimum and maximum threshold value.

After determine the optimum threshold value, the slices 2D images need to convert into 3D images. This process is called calculate 3D image in MIMICS software. In this process, we need to choose the colour of images that need to be converting into 3D images. For this study, the green colours determine the skull part of the image. Also, the quality of the 3D images can be select in MIMICS software by choose either low, medium of high quality of the images before the calculation of 3D images will be done.

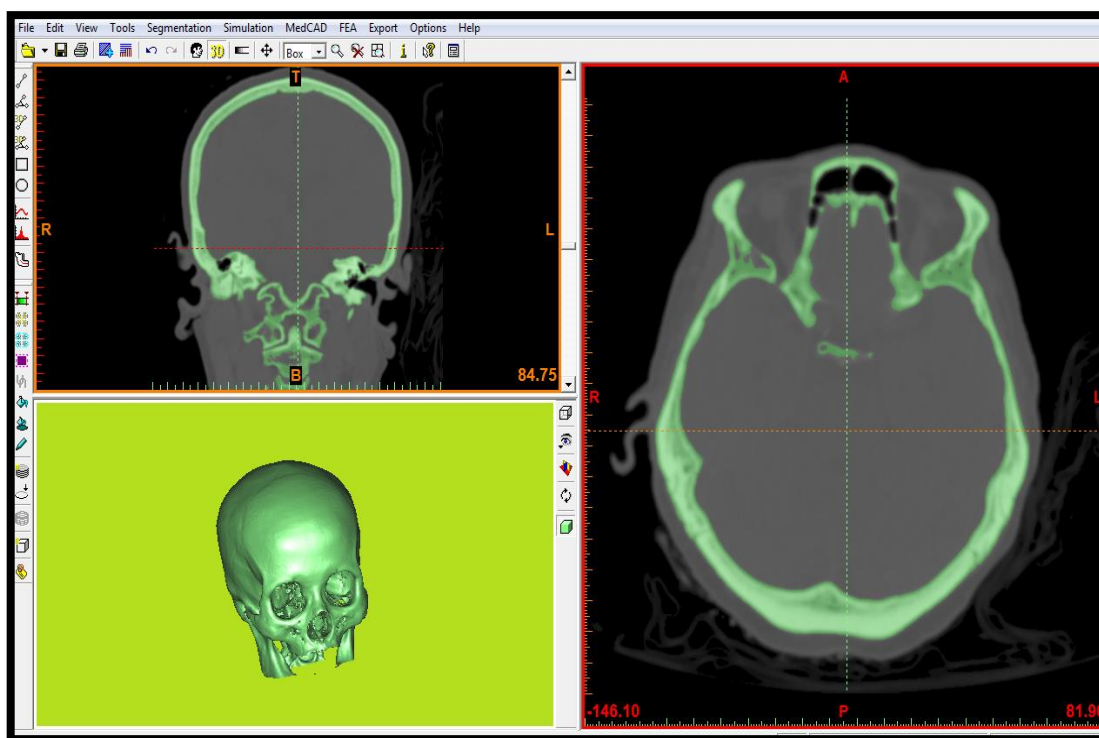


**Figure 4.5:** Calculated 3D image in MIMICS software

The figure show calculated 3D image that done by MIMICS software. From the figure, we can see that the smooth, fine and complete 3D image skull was being calculated. This is from the large number of slices and thin thickness for each layer. Then, the 3D image of human skull can be save as in other selected format file like STL, IGES, or STEP for further process like simulation by finite element analysis. Also, this MIMICS software can directly export the selected file into FEM software like Abaqus, Ansys and Pastran.

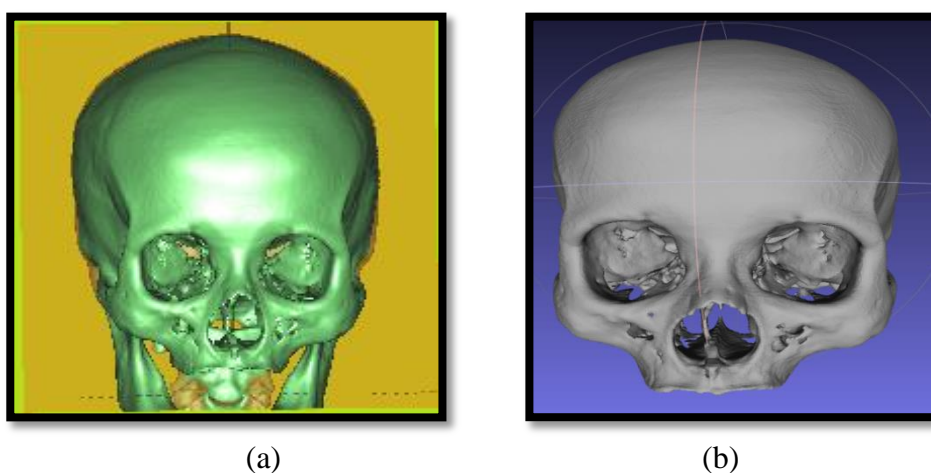


**Figure 4.6:** 3D skull model (a) 3D skull model in MIMICS 8.13 software, (b) 3D skull model in Mesh Lab software after editing and removing unnecessary part, chick bones and neck

#### **4.3 ASSESSMENT OF RACE FROM SKULL MORPHOLOGICAL FEATURES**

As discussed in previous chapter, there are three main races in the world which are Caucasoid that refer to white European, Negroid that refer black African and Mongoloid that refer to Asian. Morphology is identification process of human's fossil by comparing which features the fossil belongs to. However, this procedure cannot is not an easy matter as not all the skull features can be determine their characteristics.

One of the scopes of study is specified to Asian skull. Therefore, I need to ensure the studied skull had achieved one of the most impotent scopes of project, which is Asian skull. Therefore, regarding to this scope, recognition of which race the studied

skull belong to need to be done. For this procedure, I had compare the 3D skull model image with Caucasoid, Negroid and Mongoloid skull at three different views which are from front view, side view and lower view. As a result, the race of studied skull can be determined. However, not all the features can be clearly seen and comparable for determination procedure. For example, the nasal features, suture pattern, and zygomatic features cannot be recognising clearly. The features that can be clearly recognised like the shape of orbits, nasal sill and the base cord are enough for determine the race of the studied skull. The next sub chapter will discuss and show three different morphology features from three different races compared with studied 3D skull for assessment of race procedure.

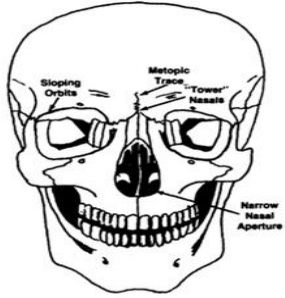
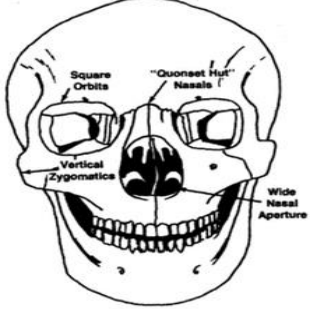
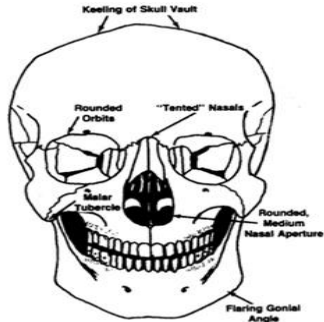
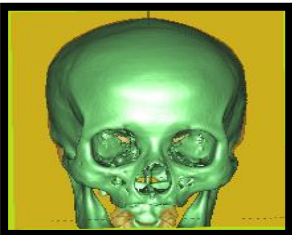
Assessment from the front view, five features can be considered which are nasal aperture, skull orbits, nasals, skull vault, and gonial while for side view, suture pattern, nasals and ramus are morphological features that can be consider and lastly, for bottom view, palate and base cord are the feature that can be consider.

The identified similarities were circled to make the comparison and assessment easier and clearly seen. Ten, the assessment will be come out with the conclusion about which race the studied 3D skull belong to.

However, from the three assessments, not all the morphological features can be recognise. Most of them cannot be recognise as they were not 3D and cannot be clearly seen. From the front view, the studied skull has similarities to Mongoloid race skull which the studied 3D skull has rounded orbits and kneeling skull vault same as Mongoloid skull, but zygomatic and nasal features cannot be clearly recognised.

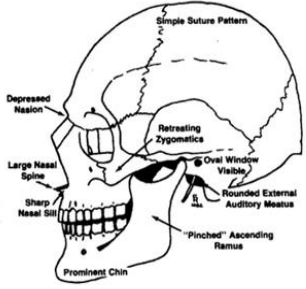
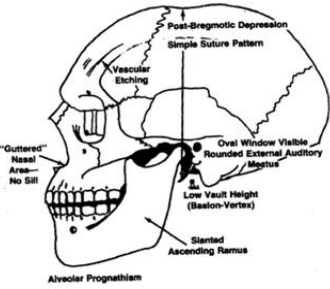
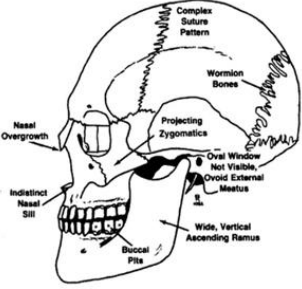
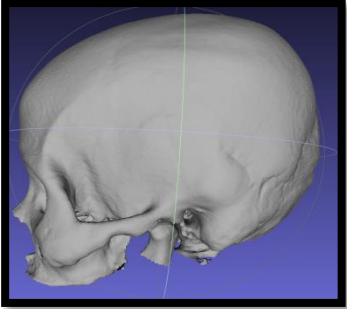
### 4.3.1 Assessment of Race from Front View Morphological Features.

Table 4.1: Assessment of Race from Front View Morphological Features.

Skull with different Race	Morphological Features
<p>Caucasoid ( White-European)</p> 	<ul style="list-style-type: none"> <li>- Sloping Orbits</li> <li>- Metopic Trace</li> <li>- “Tower” Nasals</li> <li>- Narrow Nasal Aperture</li> </ul>
<p>Negroid (Black-African)</p> 	<ul style="list-style-type: none"> <li>- Square Orbits</li> <li>- “Quoneet Hut” Nasals</li> <li>- Vertical Zygomatics</li> <li>- Wide Nasal Aperture</li> </ul>
<p>Mongoloid (Asian)</p> 	<ul style="list-style-type: none"> <li>- Keeling of Skull Vault</li> <li>- Rounded Orbits</li> <li>- “Tanted” Nasals</li> <li>- Rounded Medium Nasal Aperture</li> <li>- Flaring Gonial Angle</li> </ul>
<p>Studied 3D Skull</p> 	<ul style="list-style-type: none"> <li>- Rounded Orbits (Asian Morphological Features)</li> <li>- Keeling Skull Vault (Asian Morphological Features)</li> </ul>

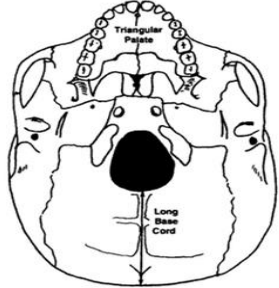
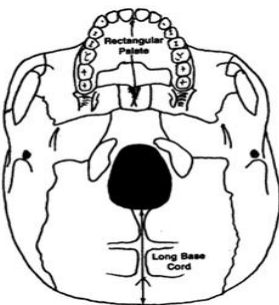
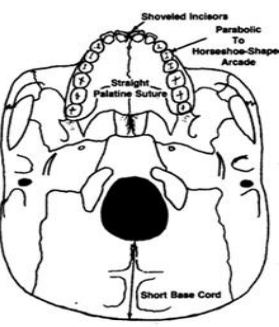
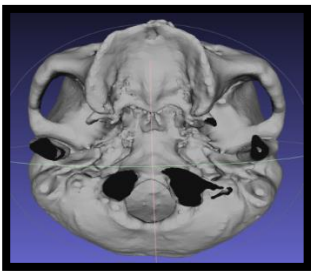
### 4.3.1 Assessment of Race from Side View Morphological Features.

**Table 4.2:** Assessment of Race from Side View Morphological Features.

Skull with different race	Morphological Features
<p>Caucasoid (White European)</p> 	<ul style="list-style-type: none"> <li>- Simple Suture Pattern</li> <li>- Depressed Nasion</li> <li>- Large Nasal Spine</li> <li>- Sharp Nasal Sill</li> <li>- Oval Window Visible</li> <li>- Rounded External Auditory Meatus</li> <li>- “Pinched” Ascending Ramus</li> </ul>
<p>Negroid ( Black-African)</p> 	<ul style="list-style-type: none"> <li>- Simple Suture Pattern</li> <li>- Vascular Etching</li> <li>- “Guttered” Nasal Area-No Sill</li> <li>- Slanted Ascending Ramus</li> <li>- Low Vault Height</li> <li>- Oval Window Visible</li> </ul>
<p>Mongoloid (Asian)</p> 	<ul style="list-style-type: none"> <li>- Complex Suture Pattern</li> <li>- Nasal Overgrowth</li> <li>- Indistinct Nasal Sill</li> <li>- Wide, Vertical Ascending Ramus</li> <li>- Oval Window Not Visible</li> <li>- Worming Bones</li> </ul>
<p>Studied 3D Skull</p> 	<ul style="list-style-type: none"> <li>- Indistinct Nasal Sill (Asian Morphological Feature)</li> <li>- Projecting Zygomatic (Asian Morphological Feature)</li> </ul>

### 4.3.1 Assessment of Race from Bottom View Morphological Features

**Table 4.3:** Assessment of Race from Bottom View Morphological Features.

Skull with Different Race	Morphological Features
Caucasoid (White-European) 	<ul style="list-style-type: none"> <li>- Triangular Palate</li> <li>- Long Base Cord</li> </ul>
Negroid ( Black African) 	<ul style="list-style-type: none"> <li>- Rectangular Palate</li> <li>- Long Base Cord</li> </ul>
Mongoloid (Asian) 	<ul style="list-style-type: none"> <li>- Shovelled Incisors Parabolic To Horseshoe - Shaped Arcade</li> <li>- Short Base Cord</li> </ul>
Studied 3D skull 	<ul style="list-style-type: none"> <li>- Short Base Cord(Asian Morphological Feature)</li> </ul>



Result of assessment from the side view can be said that the studied skull has Indistinct Nasal Sill and projecting zygomatic features which are same as Mongoloid features skull. However, nasals, nasion and ramus cannot be clearly recognised.

From the assessment from bottom view, there are the similarities of the studied 3D skull with the Mongoloid skull which they have short base cord. Unfortunately, the palate of the studied skull cannot be recognising clearly.

Therefore, we can say that the studied 3 skull has short base cord compare to Negroid and Caucasoid which have longer base cord. Also, the studied 3D skull model have Indistinct Nasal Sill compare to Negroid which have no sill and Caucasoid which have sharper nasal sill. Also, from the front view, we can see that the studied 3D skull has rounded orbits, same as Mongoloid compare to Negroid which have square orbits and Caucasoid which have sloping orbits. Obviously, the studied 3D skull has kneeling skull vault, same as Mongoloid which Negroid and Caucasoid did not have it.

In a conclusion, we can say that the studied 3D skull is an Asian skull as it has similarities with the Mongoloid human skull. For more assessment, the prototype skull model will be compare with the other three races human skull.

#### **4.4 COMPARISON OF LINEAR DIMENSION BETWEEN STUDIED SKULL AND STANDARD NORMAL SIZE ASIAN SKULL**

One of the requirements of this project is to fabricate a normal size skull. The normal skull can be ensuring by compare the size of studied skull to the average size of normal skull. This requirement is important so that the fabricated skull will not come from abnormal human with over large size of head or over small size of head. Other than that, the standard size of human skull by determines its accuracy of curvature of the skull. However, this research checks the normality of the skull by measuring its certain dimension.

There are the guides for taking the skull measurement which called skull landmarks. Skull landmarks are the specified point to point measurement that can be

taken and compare to the standard size of skull. This measurement can be done directly either by using Vernier Caliper or done in Solidworks software. The measurement using vernier calipers can be done for skull prototype model while in measurement in Solidworks can be done for 3D image of skull in STL file.

- (a) Bizygomatic Width
- (b) Bicondylar Width
- (c) Bigonal Width
- (d) Ramus Height (Right)
- (e) Ramus Height(Left)

To prevent time waste and materials waste, the measurement had been done in Solidworks software. Three times reading had been taken for each landmarks and the average calculated. There are many landmarks that can be used for skull measurement. However, for this research, only five landmarks can be consider as the other landmarks were difficult to measure in Solidworks software. The five landmarks measured are :-

The linear measurement of the studied skull will be compare with measurement of four normal Malaysian human skulls. The source of the standard size normal Malaysia human skull was from the article wrote by A.Nizam et al (2006), Dimensional Accuracy of the Skull Models Produced by Rapid Prototyping Technology Using Stereolithography Apparatus. The article wrote on how the process of accuracy of skull prototype compare to the dried original skull.

**Table 4.4:** Linear Measurement Comparison Between Studied Skull (present study) and normal size Malaysian skull (previous study)

<b>Landmarks Measurement</b>	<b>Definition</b>	<b>Mean Dimension of normal skull (mm) Source: A.Nizam et al(2006) -Average size of four normal Malaysian skull-</b>	<b>Studied Skull Measurement (mm) -Present Study-</b>	<b>Percentage Different (%)</b>
<b>Zygomatic Width ZF-ZF</b>	Distance between left and right ZF	94.07	93.967	0.12
<b>Bicondylar Width Co-Co</b>	Distance between left and right Condylion	111.58	112.481	0.8
<b>Bigonal Width Go-Go</b>	Distance between left and right Gonion	91.83	92.679	0.92
<b>Ramus Height(Left) Co-Go</b>	Distance between Condylion and Gonion (Left)	56.13	56.005	0.22
<b>Ramus Height(Right) Co-Go</b>	Distance between Condylion and Gonion (Right))	56.17	56.13	0.07

Table show the linear measurement comparison between studied 3D skull and normal size Malaysian human skull. The measurement show the percentage difference between both measurements is small. Percentage difference at bizygomatic width is 0.12%, bicondylar width is 0.8%, bigonal width is 0.92%, left ramus height is 0.22% and right ramus height is 0.07%.

As the percentage differences between the both linear measurements are small, we can conclude that the studied skull is belonging to normal size human. Therefore, the scopes of this project had been achieved and can be proceed with fabrication process.

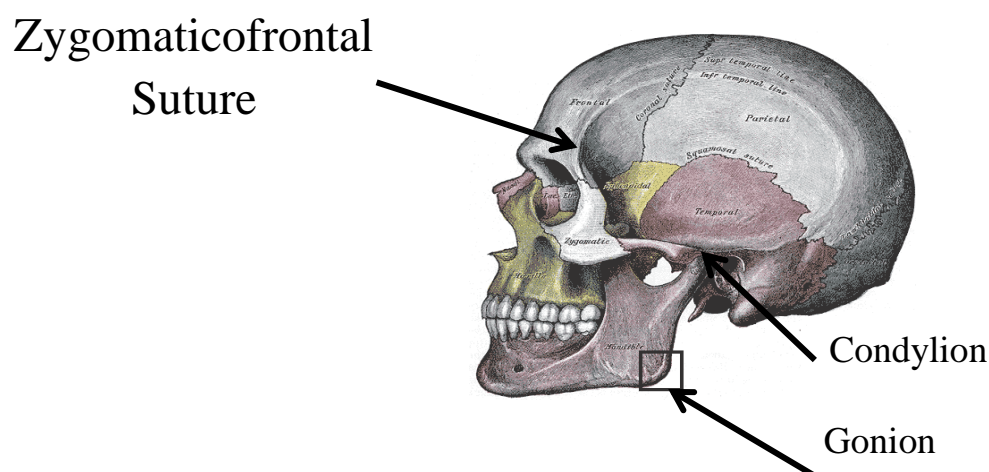


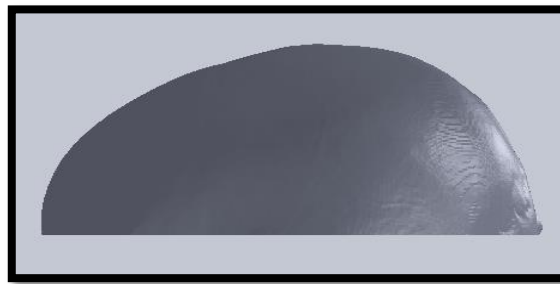
**Figure 4.7:** Skull landmarks for linear measurement

The figure shows three points that considered in the linear measurement for comparison with normal size skull. Zygomaticofrontal Suture, ZF is a point is the cranial suture between the zygomatic bone and the frontal bone. It accounts for much of the structural integrity of the skull casing. Condylion, Co is the craniometric point at the tip of the mandibular condyle and Gonion, Go is an anthropometric landmark located at the most inferior, posterior, and lateral point on the external angle of the mandible

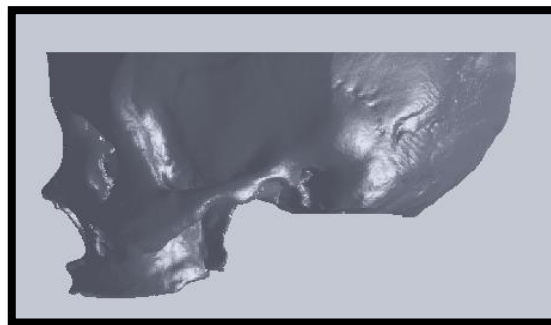
#### 4.5 THE FABRICATION OF PROTOTYPE OF NORMAL ASIAN HUMAN SKULL

As mentioned in the previous chapter, the fabrication process will be done by using Modeller Machine. Material used for this fabrication process is chemical wood or its scientific name is miraboard 700. The property of miraboard 700 is very suitable for prototype making and strong enough for testing.

As the complex shape of inner and outer part the skull, the skull was divided into two parts, upper part and lower part. Both the parts were processed separately, and then will be attaching manually together at the last phase of fabrication process. The 3D skull image was divided in MeshLab software at suitable divider line.



(a)



(b)

**Figure 4.8:** Skull Part (a) Upper part in Solidwork drawing (side view) (b) Lower part in Solidwork drawing (side view)

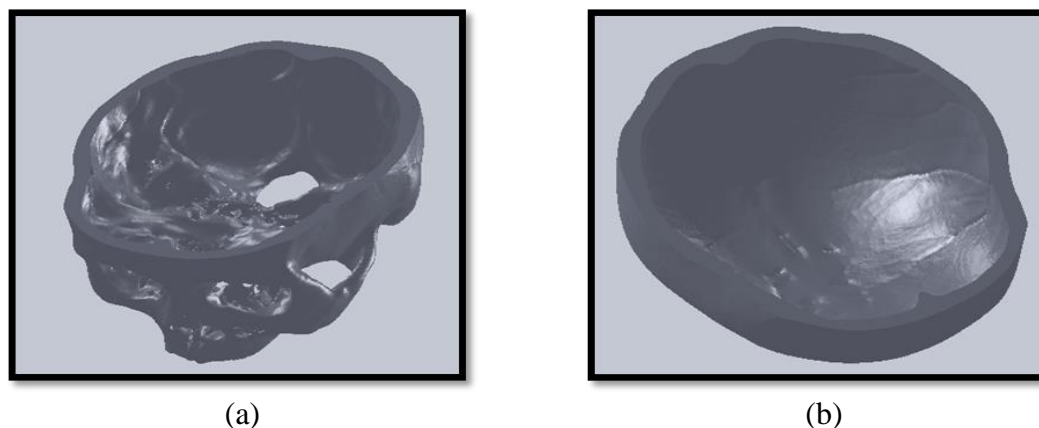


**Figure 4.9:** Isometric View (a) Isometric view of upper part, (b) Isometric view of lower part. Show complexity shape of the skull.

Before started the process, the STL file format of 3D skull image will be export to SRP software that connected to Modeller Machine. The software is used to setting the cutting of the products before estimated time of the process will appear. The five steps need to set before start the cutting processes are:

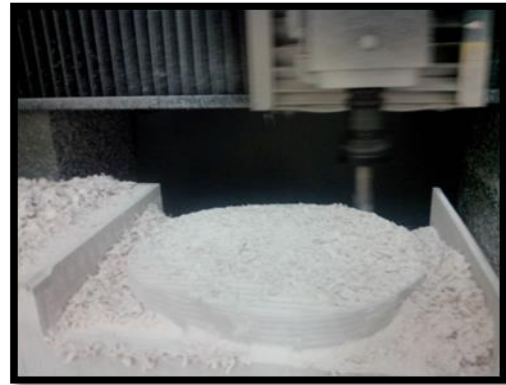
- (a) Model size and orientation
- (b) Decide what you want to do
- (c) Create the cutting data
- (d) Preview the results
- (e) Perform Cutting

First of all, we need to insert the dimension of the work piece that will be process. The width of the real product need to plus with 120mm for clamp area. Then, we need to decide on what we want to do. Generally, the process can be divide into two which are roughing and finishing. After roughing phase done, the process will automatically continue with finishing process. Before perform the cutting, the results of product need to be preview for satisfaction.

Safety factor need to be considered while the fabrication process. Safety boot, mask and goggle are compulsory to prevent any injury during the process. The estimated time for my skull prototype was about 80 hours for complete upper and lower parts of the skull prototype.



(a)



(b)



(c)



(d)



(e)



(f)

**Figure 4.10:** Cutting flow during fabricating of upper part prototype of skull



(a)



(b)



(c)



(d)



(e)



(f)

**Figure 4.11:** Cutting flow during fabricating of lower part prototype of skull



- (a) Chemical wood block was clamped and ready for cutting process
- (b) Start roughing process for each side of skull prototype, tool 10mm was used.
- (c) Start finishing process for each side of skull prototype, tool 10 mm was used
- (d) Modeller machine able to develop the complexity of the skull
- (e) Finishing process of skull prototype, tool 4mm was used.
- (f) Complete skull prototype for lower part

Unfortunately, there was an error during machining process where the created cutting data was over to its limits. This caused some defect to the face part of the prototype of skull. However, the defect was still not effect internal structure of the skull prototype, means that it will not influence the experiment result. The main structure was still in acceptable condition.

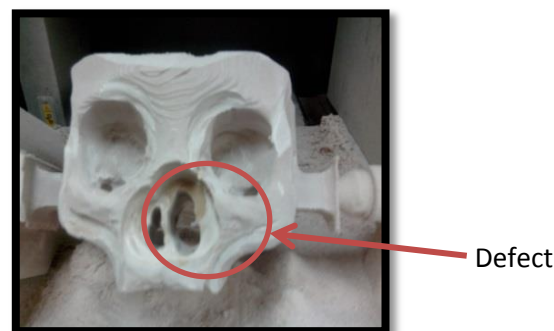


**Figure 4.12:** The defect that caused by created cutting data error

For a better result, the skull prototype was polished by using sand paper. The variability grade of the sand paper used give a fine and smooth surface of the skull prototype. At the end of fabrication process, the lower part and upper part of the skull glue together by using epoxy glue.

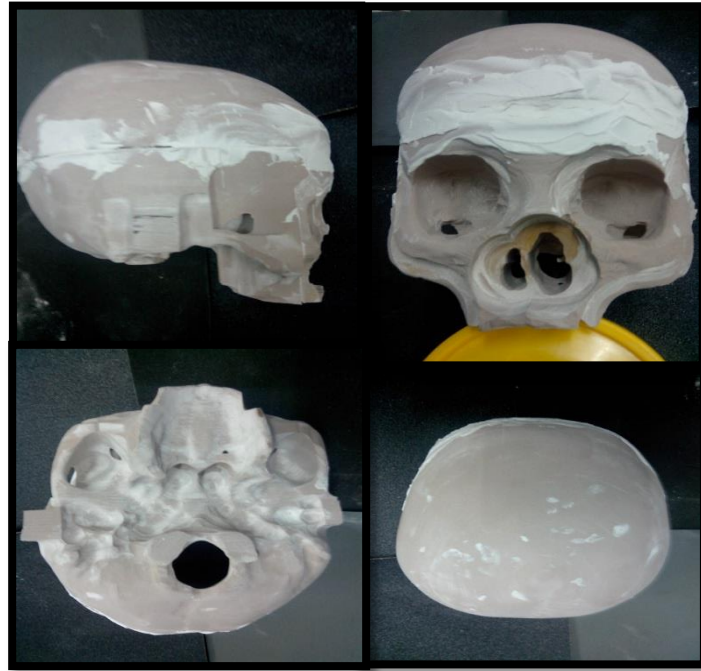


**Figure 4.13:** Complete prototype of skull

#### **4.6 CAPABILITY OF STUDIED SKULL PROTOTYPE COMPARE TO PREVIOUS STUDY**

This chapter will discuss about the capability of studied skull prototype compare to previous study. This can be determining by drop ball test experiment that had been discussed in Chapter 3. The purpose of the experiment is to study the vibration of brain after the ball was dropped on the skull at different height. Then, the result will be compare between the two skull prototype which are the rapid prototyping skull, the previous study and the wooden skull prototype, the present study.

1	DASYLab - V 10.00.01				
2	Worksheet name: DEFNAME				
3	Recording 5:58:33 PM				
4	Block length : 2000				
5	Delta : 0.000488281 sec.				
6	Number of channels : 3				
7	Measure	Write 0 [g]	Write 1 [g]	Write 2 [g]	
8	00:00.0	0.02	0.02	0.03	0.04123 5.84423
9	00:00.0	0.03	0.01	0.04	0.05099
10	00:00.0	0.03	0.02	0.04	0.05385
11	00:00.0	0.02	0.02	0.04	0.04899
12	00:00.0	0.02	0.01	0.04	0.04583
13	00:00.0	0.02	0.02	0.04	0.04899
14	00:00.0	0.02	0.01	0.04	0.04583
15	00:00.0	0.02	0.02	0.04	0.04899
16	00:00.0	0.03	0.01	0.04	0.05099
17	00:00.0	0.02	0.02	0.04	0.04899
18	00:00.0	0.02	0.02	0.03	0.04123
19	00:00.0	0.02	0.01	0.04	0.04583
20	00:00.0	0.02	0.02	0.04	0.04899
21	00:00.0	0.02	0.01	0.03	0.03742
22	00:00.0	0.03	0.01	0.04	0.05099
23	00:00.0	0.02	0.02	0.04	0.04899
24	00:00.0	0.02	0.02	0.04	0.04899
25	00:00.0	0.03	0.01	0.04	0.05099
26	00:00.0	0.02	0.01	0.04	0.04583
27	00:00.0	0.02	0.02	0.04	0.04899
28	00:00.0	0.02	0.01	0.04	0.04583
29	00:00.0	0.03	0.01	0.03	0.04359
30	00:00.0	0.03	0.01	0.04	0.05099
31	00:00.0	0.02	0.01	0.03	0.03742
32	00:00.0	0.03	0.01	0.04	0.05099
33	00:00.0	0.03	0.02	0.04	0.05385

**Figure 4.14:** Raw data from DASYLab signal process

The figure show raw data obtained from DASYLab signal process which the data come out with time and vibration of brain variables. From the raw data, the resultant acceleration was calculated.

The graph below show the vibration versus time result at 0.5m height distance from the ball to the skull. From the graph, we can see that the brain vibrate at maximum rate which is 5.844228g or 57.3318 m/s<sup>2</sup> when the skull contact to the skull and continue vibrate after the contact time.

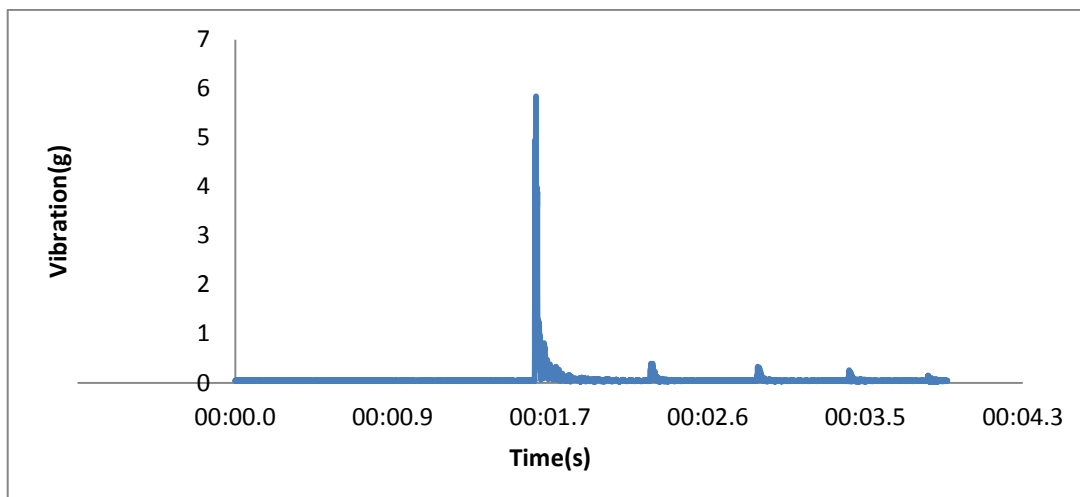


**Figure 4.15:** Vibration versus time at 0.5m height

For an accurate result, the experiment was repeated three times at each height, and the average was calculated as below.

**Table 4.5:** Result of vibration at different height: ABS prototype skull model

Height from ball to skull (m)	Average of vibration (g)
0.5	5.78
1.0	9.33
1.5	12.93

**Table 4.6:** Result of vibration at different height: Miraboard 700 prototype skull model

Height from ball to skull (m)	Average of vibration (g)
0.5	4.22
1.0	8.01
1.5	11.75

To determine the correlation between the vibration of the brain and the height of the ball to skull, the graph vibration versus height of ball to skull was plotted. The graph show that the higher the distance between the ball and the skull, the higher the vibration of the brain. This is caused by the distance of the ball to the brain will influence the velocity of the ball.

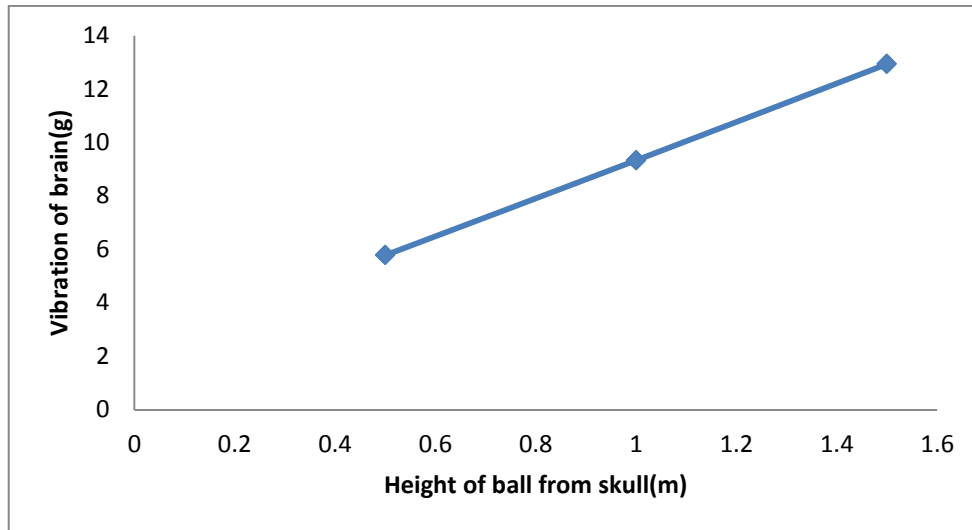


**Figure 4.16:** Height of ball from skull versus vibration (ABS skull prototype)

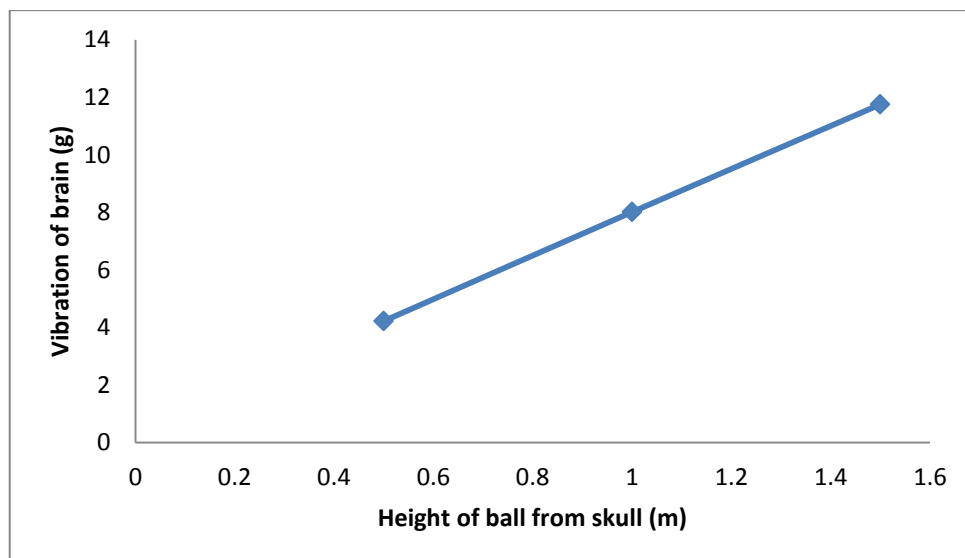


**Figure 4.17:** Height of ball from skull versus vibration (Miraboard 700 skull prototype)

The velocity equation shows that the speed is directly proportional to the distance. Therefore, we can say that the higher distance the between ball and skull, the higher the speed or velocity.

The acceleration equation prove the correlation of the graph which the height of ball to skull will influence the brain vibration. The higher distance between ball and skull, the vibration or acceleration of the brain will be higher.

In order to compare the result between the two skulls for determination of capability of studied 3D skull model, both results were compared.

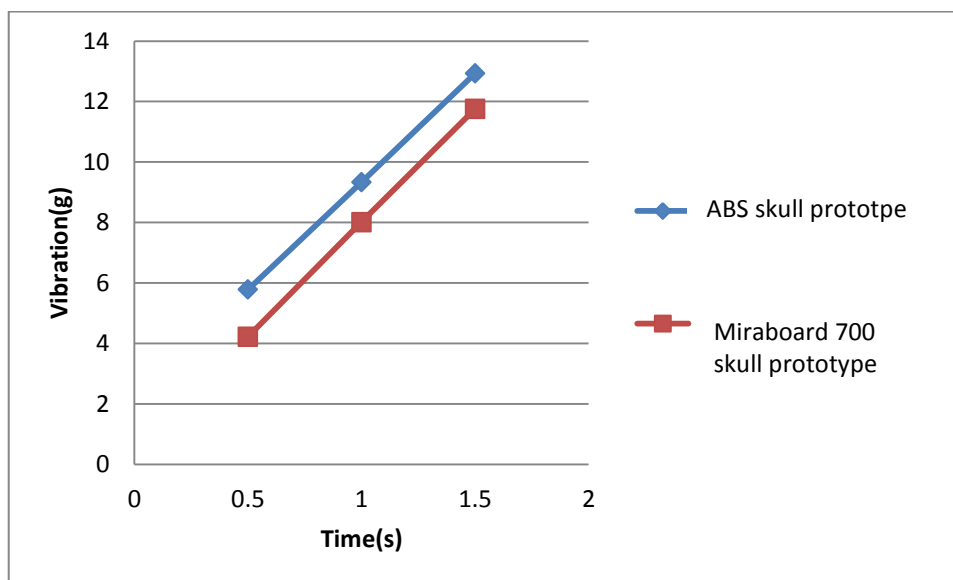


**Figure 4.18:** Comparison between previous study of skull and present study of skull

The main factor that caused the difference between the two model vibration results was because of their material difference. Acrylonitrile butadiene styrene (ABS), material for previous study skull has higher density than miraboard 700. This means that the ABS skull prototype has higher mass compare to miraboard 700 skull prototype. The higher the mass, the higher the momentum occurs outside the skull cause more vibration occur on the surface of ABS skull prototype. The miraboard skull prototype which has lighter weight has an ability to absorb force that occur at its surface cause the transferred vibration inside the ecogel 200 is less. The percentage difference between the two different materials for skull prototype is 27%.

Other than experiment, the comparison between the two different material of skull also determined by calculation by using implicit expression that was derived by (Young,2003) from which the impact characteristics can straightforwardly be solved, by introducing further approximations into the model explicit expressions for the impact characteristics were obtained as given here in Eq. (4.1)

$$F_{max} = \frac{R *_{\frac{1}{5}} E *_{\frac{2}{5}} m *_{\frac{3}{5}} \Delta v_{\frac{6}{5}} E_{sh}^1 h}{\left(\frac{1}{\sqrt{2.3}}\right) R *_{\frac{1}{5}} E *_{\frac{2}{5}} m *_{\frac{1}{10}} \Delta v_{\frac{1}{5}} R_{sh}^1 (1 - v_{sh}^2)^{\frac{1}{4}} + \left(\sqrt{\frac{3}{2}}\right) \left(\frac{16}{15}\right)^{\frac{1}{10}} E_{sh}^1 h}$$

Eq(4.1)

$$\frac{1}{R *} = \frac{1}{R_{sh}} + \frac{1}{R_{sol}}$$

$$\frac{1}{m *} = \frac{1}{m_{sh}} + \frac{1}{m_{sol}}$$

$$\frac{1}{E *} = \frac{1 - v_{sh}^2}{E_{sh}} + \frac{1 - v_{sol}^2}{E_{sol}}$$

Where  $R_{sh}$  and  $R_{sol}$  represent outer radius of skull and ball respectively and  $E_{sol}$ ,  $E_{sh}$  and  $v_{sol}$ ,  $v_{sh}$  are the Young's moduli and Poisson's ratio of shell and solid, respectively. For this comparison, some material properties of miraboard 700 and ABS need to be determined.

**Table 4.7:** Material Properties for skull prototype

<b>Material</b>	<b>Miraboard700 (Chemical Wood)</b>	<b>Acrylonitrile butadiene styrene (ABS),</b>	<b>Ball (Butyl Rubber)</b>
Poisson ratio, $\nu$	0.2	0.35	0.499
Young Modulus, E(GPa)	10	2.3	0.1
Mass, m (kg)	0.525	0.735	0.4251
Thickness, h (mm)	8	5	-
Radius, R (mm)	71	76	112

For miraboard 700,

$$\frac{1}{R^*} = \frac{1}{71} + \frac{1}{112}$$

$$R^* = 43.454\text{mm}$$

$$\frac{1}{m^*} = \frac{1}{0.4251} + \frac{1}{0.525}$$

$$m^* = 0.2349\text{kg}$$

$$\frac{1}{E^*} = \frac{1 - 0.499^2}{0.1} + \frac{1 - 0.2^2}{11}$$

$$E^* = 0.132 \text{ Gpa}$$



$F_{max}$

$$= \frac{43.454^{\frac{1}{5}} 0.132^{\frac{2}{5}} 0.2349^{\frac{3}{5}} 0.299^{\frac{6}{5}} 10^{\frac{1}{2}} 8}{\left(\frac{1}{\sqrt{2.3}}\right) 43.454^{\frac{1}{5}} 0.132^{\frac{2}{5}} 0.2349^{\frac{1}{10}} 0.299^{\frac{1}{5}} 71^{\frac{1}{2}} (1 - 0.2^2)^{\frac{1}{4}} + \left(\sqrt{\frac{3}{2}}\right) \left(\frac{16}{15}\right)_{10}^1 10^{\frac{1}{2}} 8}$$

$$F_{max} = 0.089 \text{ N}$$

For ABS,

$$\frac{1}{R^*} = \frac{1}{76} + \frac{1}{112}$$

$$R^* = 45.277 \text{ mm}$$

$$\frac{1}{m^*} = \frac{1}{0.4251} + \frac{1}{0.735}$$

$$m^* = 0.2693 \text{ kg}$$

$$\frac{1}{E^*} = \frac{1 - 0.499^2}{0.1} + \frac{1 - 0.35^2}{2.3}$$

$$E^* = 0.1269 \text{ Gpa}$$

$F_{max}$

$$= \frac{45.277^{\frac{1}{5}} 0.1269^{\frac{2}{5}} 0.2693^{\frac{3}{5}} 0.149^{\frac{6}{5}} 2.3^{\frac{1}{2}} 5}{\left(\frac{1}{\sqrt{2.3}}\right) 45.277^{\frac{1}{5}} 0.1269^{\frac{2}{5}} 0.2693^{\frac{1}{10}} 0.149^{\frac{1}{5}} 76^{\frac{1}{2}} (1 - 0.35^2)^{\frac{1}{4}} + \left(\sqrt{\frac{3}{2}}\right) \left(\frac{16}{15}\right)_{10}^1 2.3^{\frac{1}{2}} 5}$$

$$F_{max} = 0.134 \text{ N}$$

## 4.7 CONCLUSION

From the implicit expression (Young, 2003), maximum force for miraboard 700 is 0.069N compare to ABS skull prototype, the maximum force is 0.134N. The percentage difference between the two different materials is 33.58%. The percentage difference may cause by different Young Modulus and thickness of the skull prototype. ABS skull prototype which have less thickness compare to miraboard 700 will absorb more vibration to the ecogel 200 and cause higher value of vibration that occur at brain. In a conclusion for this chapter, the research has valid result for experiment as the percentage value for experiment which is 27% and percentage different for analytical method is 33%.

## **CHAPTER 5**

### **CONCLUSION AND RECOMMENDATION**

#### **5.1 INTRODUCTION**

After completing all the tasks required to fulfil the scope of project, some important concluding remarks and future recommendations are discussed in this last chapter. This chapter summarized the conclusions and recommendations for the overall objective of the project

#### **5.2 CONCLUSION**

Firstly, the conclusion is about the prototype of the human skull. The developed skull prototype had achieve overall of the scope research which are the skull prototype must have morphological features of Asian skull with normal size human skull. This skull prototype was able to develop and achieve its scope because the raw data, CT scan images was originally from Malaysian. In order to ensure its morphological features match an Asian human skull morphology feature, the 3D image of the skull was compared with the other three races of skull which are Caucasoid ( White-European), Negroid (Black European) and Mongoloid (Asian). From the assessment of race from skull morphological features, the studied 3D skull can be clarify as Asian skull as there were many similarities of its features to Mongoloid features. Other than that, the linear dimension measurement had been done in order to ensure that the studied 3D skull was

belonging to normal size skull. Then, the comparison of linear measurement between the present study skull and standard size of normal skull had found out that the skull was normal in size. Then, the project proceeds with fabrication process.

Secondly, the conclusion is about the capability of the skull prototype. From the drop ball experiment, the vibration occur inside ecogel of miraboard 700 is less compare to ABS skull prototype caused by different materials of both skulls. The different material of both skull cause the different force absorb by the ecogel 200 that replace brain inside the skull prototype. The result of drop ball experiment validated by analytical method which have almost the same percentage different value to the experiment results.

### **5.3 RECOMMENDATION FOR FUTURE WORK**

For further research, the skull prototype should complete with prototype of brain with actual size and shape of brain so that the result from experiment will be more accurate. Other than that, the skull prototype should be varying in gender, age and races so that the differences between the gender and age can be determine and study. This can be achieve by vary the raw data of CT scan images. Collaboration with hospitals should be achieved for more raw data sources. Lastly, in order to prevent any defect of skull prototype, the fabrication process should be done by using rapid prototyping machine that able to produce harder, more accurate and better products.

## REFERENCES

This guide is prepared based on the following references:

- M. O'Neil, B.Khambay, K.F.Moos, J. Barbenel, F.Walker, A.Ayoub (2010),  
*"Validation of a new method for building a three dimensional physical model of the skull and dentition"* British Journal of Oral Maxillofacial surgery 50(2012) 49-54
- Christoph P.E. Zollikofer and Marcia S. Ponce de Leon University of Zurich(1995)  
*"Tools for Rapid Prototyping in the Bioscience"*
- Chung-Shing Wang, Wei-Hua A.Wang, Man-Ching Lin (2009) "*STL rapid prototyping bio-CAD model for CT medical image segmentation*" Computers in Industry 61 (2010) 187-197
- A.Nizam, R.N Gopal, L.Naing, A.B Hakim, A.R Samsudin (2006) "*Dimensional Accuracy of the Skull Models Produced by Rapid Prototyping Technology Using Stereolithograph Apparatus*" Archives of Orofacial Sciences 2006; 1:60-66
- Daniel J.Kelley, Farhoud M, Meyerand M.E, Nelson D.L, Ramirez L.F, Dempsy R.J, Wolf A.J, Alexendar A.L, Davidson R.J (2007), "*Creating Physical 3D Stereolithograph Models of Brain and Skull*"
- C.Van Lierde, T. Huysmans, B.Depreitere, J.Vander Sloten, R. Van Audekercke, G.Van der Perre, J. Goffin, (2002) "*Curvature Accuracy of RP Models*"
- Jorg Scheneider, Rene Decker, Willi A.Kalender (2002) "*Accuracy in Medical Modelling*)
- J Asami, N Kawai, Y Honda, H Shigehara, T Wakasa and K Kishi (2001) "*Comparison of three-dimensional computed tomography with rapid prototype models in the management of coronoid hyperplasia*" Dentomaxillofacial Radiology (2001) 30, 330 ± 335
- E.A.C. Johnson and P.G. Young(2005) "*On the use of a patient-specific rapid-prototyped model to simulate the response of the human head to impact and comparison with analytical and finite element models*"**38**(1)
- J.Veleminska, J.Bruzek, P.Veleminsky, L.Bigoni, A.Sefcakova and S.Katina (2007) "*Variability of the Upper Paleolithic skulls from Czech Republic: Craniometric comparison with recent human standards*"**59**(1)

S.G.M. Hossain(2010) "*Material Modeling and Analysis for the Development of a Realistic Blast Headform,*"

# APPENDIX A1 : RAW DATA CT SCAN IMAGES

The screenshot displays the 'Organize Images' window. At the top, it shows 'Images in project, 176 selected:'. Below this is a list of image positions from 0 to 40, each with a red checkmark in the 'Project' column. The main area is a grid of 40 axial CT scan slices, each labeled with its position number. The interface includes a 'Select All' dropdown menu, a 'Preview' checkbox, and a 'Contrast' section with radio buttons for 'Current', 'CT', and 'MR'. There are also input fields for 'Minimum: 1024' and 'Maximum: 1862'. At the bottom right, there are 'Add' and 'Remove' buttons, and a 'Skip images:' dropdown menu set to 'Custom'. The 'Preview size:' dropdown is set to 'Medium'. The window title bar reads 'Organize Images'.

Nr	Project	Position
0	✓	0.79483
1	✓	1.79483
2	✓	2.79483
3	✓	3.79483
4	✓	4.79483
5	✓	5.79483
6	✓	6.79483
7	✓	7.79483
8	✓	8.79483
9	✓	9.79483
10	✓	10.7948
11	✓	11.7948
12	✓	12.7948
13	✓	13.7948
14	✓	14.7948
15	✓	15.7948
16	✓	16.7948
17	✓	17.7948
18	✓	18.7948
19	✓	19.7948
20	✓	20.7948
21	✓	21.7948
22	✓	22.7948
23	✓	23.7948
24	✓	24.7948
25	✓	25.7948
26	✓	26.7948
27	✓	27.7948
28	✓	28.7948
29	✓	29.7948
30	✓	30.7948
31	✓	31.7948
32	✓	32.7948
33	✓	33.7948
34	✓	34.7948
35	✓	35.7948
36	✓	36.7948
37	✓	37.7948
38	✓	38.7948
39	✓	39.7948
40	✓	40.7948

### APPENDIX A2 : RAW DATA CT SCAN IMAGES

Organize Images

Images in project, 176 selected:

Nr	Project	Position
0	✓	0.79483
1	✓	1.79483
2	✓	2.79483
3	✓	3.79483
4	✓	4.79483
5	✓	5.79483
6	✓	6.79483
7	✓	7.79483
8	✓	8.79483
9	✓	9.79483
10	✓	10.7948
11	✓	11.7948
12	✓	12.7948
13	✓	13.7948
14	✓	14.7948
15	✓	15.7948
16	✓	16.7948
17	✓	17.7948
18	✓	18.7948
19	✓	19.7948
20	✓	20.7948
21	✓	21.7948
22	✓	22.7948
23	✓	23.7948
24	✓	24.7948
25	✓	25.7948
26	✓	26.7948
27	✓	27.7948
28	✓	28.7948
29	✓	29.7948
30	✓	30.7948
31	✓	31.7948
32	✓	32.7948
33	✓	33.7948
34	✓	34.7948
35	✓	35.7948
36	✓	36.7948
37	✓	37.7948
38	✓	38.7948
39	✓	39.7948
40	✓	40.7948

Select All  
Unselect All  
 Preview  
- Contrast  
 Current  
 CT  
 MR  
Minimum: 1024  
Maximum: 1862

Add Remove

Preview size: Medium Skip images: Custom



### APPENDIX A3 : RAW DATA CT SCAN IMAGES

Organize Images

Images in project, 176 selected:

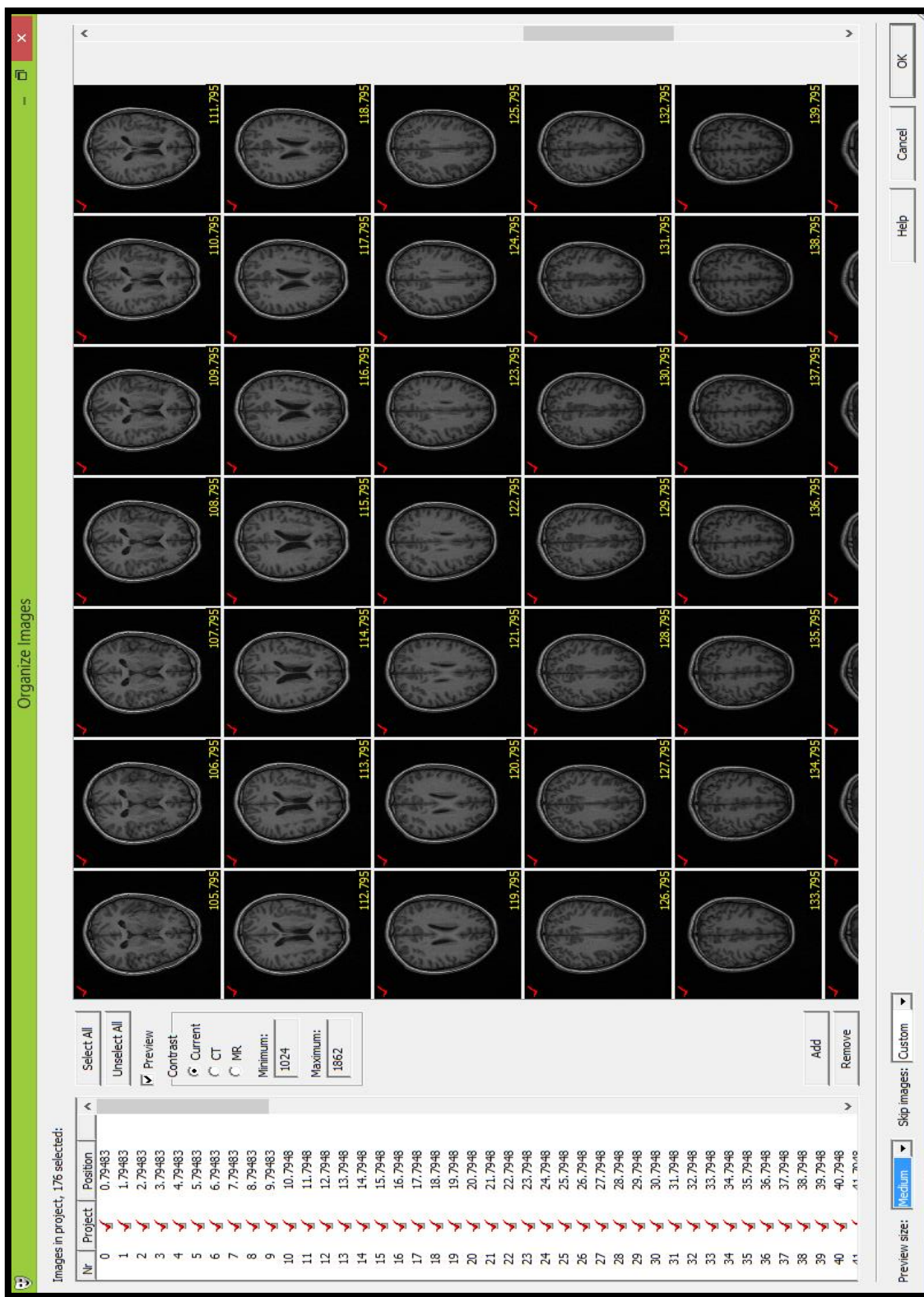
Nr	Project	Position
0	✓	0.79483
1	✓	1.79483
2	✓	2.79483
3	✓	3.79483
4	✓	4.79483
5	✓	5.79483
6	✓	6.79483
7	✓	7.79483
8	✓	8.79483
9	✓	9.79483
10	✓	10.7948
11	✓	11.7948
12	✓	12.7948
13	✓	13.7948
14	✓	14.7948
15	✓	15.7948
16	✓	16.7948
17	✓	17.7948
18	✓	18.7948
19	✓	19.7948
20	✓	20.7948
21	✓	21.7948
22	✓	22.7948
23	✓	23.7948
24	✓	24.7948
25	✓	25.7948
26	✓	26.7948
27	✓	27.7948
28	✓	28.7948
29	✓	29.7948
30	✓	30.7948
31	✓	31.7948
32	✓	32.7948
33	✓	33.7948
34	✓	34.7948
35	✓	35.7948
36	✓	36.7948
37	✓	37.7948
38	✓	38.7948
39	✓	39.7948
40	✓	40.7948
41	✓	41.7948

Select All  
Unselect All  
Preview  
Contrast  
Current  
CT  
MR  
Minimum: 1024  
Maximum: 1862

Add  
Remove

Preview size: Medium Skip images: Custom

APPENDIX A4 : RAW DATA CT SCAN IMAGES



APPENDIX A5 : RAW DATA CT SCAN IMAGES

Organize Images

Images in project, 176 selected:

Nr	Project	Position
0	✓	0.79483
1	✓	1.79483
2	✓	2.79483
3	✓	3.79483
4	✓	4.79483
5	✓	5.79483
6	✓	6.79483
7	✓	7.79483
8	✓	8.79483
9	✓	9.79483
10	✓	10.7948
11	✓	11.7948
12	✓	12.7948
13	✓	13.7948
14	✓	14.7948
15	✓	15.7948
16	✓	16.7948
17	✓	17.7948
18	✓	18.7948
19	✓	19.7948
20	✓	20.7948
21	✓	21.7948
22	✓	22.7948
23	✓	23.7948
24	✓	24.7948
25	✓	25.7948
26	✓	26.7948
27	✓	27.7948
28	✓	28.7948
29	✓	29.7948
30	✓	30.7948
31	✓	31.7948
32	✓	32.7948
33	✓	33.7948
34	✓	34.7948
35	✓	35.7948
36	✓	36.7948
37	✓	37.7948
38	✓	38.7948
39	✓	39.7948
40	✓	40.7948

Select All  
Unselect All  
Preview  
Contrast  
Current  
CT  
MR  
Minimum: 1024  
Maximum: 1862

119.795 120.795 121.795 122.795 123.795 124.795 125.795  
126.795 127.795 128.795 129.795 130.795 131.795 132.795  
133.795 134.795 135.795 136.795 137.795 138.795 139.795  
140.795 141.795 142.795 143.795 144.795 145.795 146.795  
147.795 148.795 149.795 150.795 151.795 152.795 153.795

Preview size: Medium Skip images: Custom Add Remove

Help Cancel OK

APPENDIX A6 : RAW DATA CT SCAN IMAGES

Organize Images

Images in project, 176 selected:

Nr	Project	Position
0	✓	0.79483
1	✓	1.79483
2	✓	2.79483
3	✓	3.79483
4	✓	4.79483
5	✓	5.79483
6	✓	6.79483
7	✓	7.79483
8	✓	8.79483
9	✓	9.79483
10	✓	10.7948
11	✓	11.7948
12	✓	12.7948
13	✓	13.7948
14	✓	14.7948
15	✓	15.7948
16	✓	16.7948
17	✓	17.7948
18	✓	18.7948
19	✓	19.7948
20	✓	20.7948
21	✓	21.7948
22	✓	22.7948
23	✓	23.7948
24	✓	24.7948
25	✓	25.7948
26	✓	26.7948
27	✓	27.7948
28	✓	28.7948
29	✓	29.7948
30	✓	30.7948
31	✓	31.7948
32	✓	32.7948
33	✓	33.7948
34	✓	34.7948
35	✓	35.7948
36	✓	36.7948
37	✓	37.7948
38	✓	38.7948
39	✓	39.7948
40	✓	40.7948
41	✓	41.7948

Select All:  Unselect All

Preview

Contrast:  Current  CT  MR

Minimum: 1024

Maximum: 1862

Add

Remove

Preview size: Medium | Skip images: Custom

Help | Cancel | OK

**APPENDIX B1 : GANTT CHART FYP 1**

PROJECT PROGRESS	SEMESTER 1														
	WEEKS														
	1	2	3	4	5	6	7	8	9	10	11	12	13	14	15
1. Introduction and briefing about the project	■	■	■												
	■	■	■												
2. Determine objective and scope			■	■											
			■	■	■										
3. Find the related information from journals		■	■	■	■	■	■	■	■	■	■	■	■	■	■
		■	■	■	■	■	■	■	■	■	■	■	■	■	■
4. Do research and collect the suitable information				■	■	■	■	■	■	■	■	■	■	■	■
				■	■	■	■	■	■	■	■	■	■	■	■
5. Setup experiment and methodology part						■	■	■	■	■	■	■	■	■	■
						■	■	■	■	■	■	■	■	■	■
6. Run the experiment for a few subjects										■	■	■	■	■	■
										■	■	■	■	■	■
7. Prediction on initial finding and result analysis												■	■	■	■
												■	■	■	■
8. Report writing and presentation														■	■
														■	■

 **Planning**

 **Actual**

**APPENDIX B2 : GANTT CHART FYP 2**

PROJECT PROGRESS	SEMESTER 2														
	WEEKS														
	1	2	3	4	5	6	7	8	9	10	11	12	13	14	15
1. Get CT scan data images	■	■	■	■	■	■									
	■	■	■	■	■	■	■								
2. Fabrication Process						■	■	■	■						
								■	■	■	■	■	■		
3. Drop Ball Experiment							■	■	■	■					
													■	■	
4. Data analysis									■	■	■	■	■		
										■	■	■	■	■	
5. Results discussion and conclusion										■	■	■	■	■	
										■	■	■	■	■	
6. Report writing										■	■	■	■	■	
											■	■	■	■	
7. Presentation															■
															■

■ Planning

■ Actual